6-2006

The synthesis and characterization of a metal complex containing chemically non-equivalent axial cyanide ligands

Derek D. Waymand
Union College - Schenectady, NY

The Synthesis and Characterization of a Metal Complex Containing Chemically Non-Equivalent Axial Cyanide Ligands

By

Derek Wayman

****

Submitted in partial fulfillment
of the requirements for
Honors in the Department of Chemistry

Union College

June, 2006

ABSTRACT

WAYMAN, DEREK The Synthesis and Characterization of a Chemically Non-Equivalent Dicyano Transition Metal Complex With an Emphasis on ^{13}C NMR spectroscopy. Department of Chemistry, June 2006.

In order to analyze the magnitude and factors which effect ^{13}C-^{13}C NMR coupling through a metal center, we have synthesized an octahedral dicyano cobalt (III) complex in which two trans cyanides are chemically non-equivalent. Although similar complexes have been reported, their spectroscopic characterization with isotopically labeled cyanide ($^{13}CN^-$) has yet to be studied in detail. To date, the complex $(Et_4N)_2[Co(PyPS(SMe))(^{12}CN)_2]$ has been isolated and characterized by ^1H and ^{13}C NMR on both 200 and 500 MHz field strengths. The NMR spectra have shown the complex to have hindered rotation around the pendant thioether arm which renders the complex asymmetric. Also isolated was the isotopically labeled complex $(Et_4N)_2[Co(PyPS(SMe))(^{13}CN)_2]$. This complex was characterized on both 200 and 500 MHz NMR instruments and showed considerable ^{13}C-^{13}C interactions through the cobalt (III) metal center. The interactions gave rise to two doublets centered near 140.1 and 137.5 ppm. Additional temperature dependant studies were performed on the complex in the range of 20 °C – 45 °C on a 500 MHz instrument to probe the barrier to rotation of the pendant thioether. In order to confirm the interactions were from ^{13}CN / ^{13}CN, three 50 % ^{13}CN and 50 % ^{12}CN complexes were isolated. Finally, in depth theoretical coupling constants calculations have been performed on the isotopically labeled dicyano complex which are remarkably close to the experimental values.

Introduction

Nuclear Magnetic Resonance (NMR) Spectroscopy has found wide use in nearly all fields of chemistry in the characterization and analysis of many different types molecules. The broad range of studies that can be performed and the incredible amount of information that can be obtained via NMR spectroscopy makes it a very powerful resource in chemical studies. The basic principles of NMR spectroscopy will first be discussed before a detailed description of its applications and the current research are presented.

NMR spectroscopy Concepts

The underlying principle behind NMR spectroscopy is that a nucleus with an overall magnetic spin will have its energy levels split when placed in an NMR instrument. This happens because the nucleus aligns itself either with or against the magnetic field. There are only certain nuclei that are actually NMR active. The most commonly studied nuclei are the ^{1}H nucleus and the ^{13}C nucleus, although other NMR active nuclei include ^{9}Be, ^{10}B, ^{11}B, ^{14}N, ^{15}N, ^{17}O, ^{19}F, ^{27}Al, ^{29}Si, ^{31}P, and ^{59}Co. The splitting of energy levels is what gives rise to the NMR signal that is observed.

NMR instrumentation is based on the induced transitions between the magnetic energy levels, known as the Zeeman Energy Levels. When a sample is placed into an NMR magnet, a variable radio frequency (RF) is then applied to it. When equal to the Zeeman energy transition, the RF splits the energy levels of the sample (brings them into resonance with the magnetic field) and thus gives rise to the NMR signal.

In Fourier Transform Spectroscopy which is used in our lab, a broad band, short RF is used to excite a wide range of nuclei in the sample. The NMR active nuclei in the sample will absorb the RF characteristic of their resonance. The NMR detector will then measure the Free Induction Decay (FID) of the resonating nuclei as they return to the ground spin state. The FID is related to the frequency at which the nucleus resonates.[1]

The theory described above if for an individual, *free*, NMR active nucleus. However, it is almost always the case in a more applicable situation that a sample has multiple "types" of atoms bonded together, each being NMR active and having NMR active nuclei bonded to it. In addition to the other bound NMR active nuclei, there are also surrounding electron clouds which are capable of affecting an NMR active nucleus. Chemical shift and spin-spin splitting, the most widely observed properties of NMR spectra are a result of the interactions of surrounding NMR active nuclei and surrounding electron clouds.[1]

Chemical Shift

The chemical shift of an NMR active nucleus is due to its interaction witb the chemical species in the nuclei's immediate vicinity and is represented on a spectrum in parts per million (ppm). The ppm label is a unit which is related to the frequency at which the nuclei resonate. The chemical shift of a given NMR active nucleus is a result of the interaction of the surrounding nuclei and electron clouds. Since these interactions can vary, the chemical shifts of nuclei in different chemical environments vary. The first factor that affects the chemical shift is shielding. Shielding is related to the amount of influence imparted by the magnetic field of the surrounding electron clouds and nuclei.

Differences in shielding are reflected in differences in chemical shift. With increased surrounding electron density, the nucleus "feels" less of the external magnetic field and the nucleus is termed more shielded. This causes the chemical shift to move upfield (closer to zero), or toward the right on an NMR spectrum. The upfield shift means that a larger applied energy is required (via the variable RF frequency) in order to bring the NMR active nuclei into resonance. Conversely, nuclei which are near electron withdrawing substituents or which are in aromatic systems are termed deshielded. These chemical shifts will be located downfield, or to the left of an NMR spectrum. The reason for this downfield shift is case dependant. An electron withdrawing substituents effectively "pulls" electron density away from a nucleus, allowing it to be more exposed to the external magnetic field. In an aromatic system, the ring current of the delocalized pi electrons creates a magnetic field which is oriented in the direction of the external magnetic field. Therefore, the NMR active nuclei "feel" the magnetic field created by the ring current in addition to the external magnetic field.[1] In both cases, there is a downfield shift which is due to the fact that less energy (weaker applied variable RF frequency) has to be applied to the nucleus to bring it into resonance. Figure 1 shows a sample spectrum of ethylbenzene which demonstrates the concept of chemical shift. As noted by the arrows, the chemical shift for the peak which corresponds to the terminal CH_3 is the farthest upfield, because it is neither involved in a delocalized pi system or next to an electron withdrawing group. Shifted 1.5 ppm from the CH_3 group is the CH_2. This downfield shift of the CH_2 is due to its closer proximity to the phenyl ring and is therefore pushed downfield. Finally, at 7.1 ppm is the series of peaks that corresponds to the five aromatic protons on the phenyl ring.

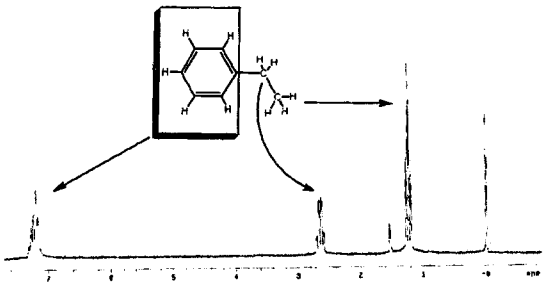

Figure 1. A sample ^{1}H NMR spectrum of ethylbenzene with annotations to indicate the position of the peaks of the relative hydrogens. The Figure illustrates the differences observed in the chemical shifts of various protons on the molecule.

Nuclei in different chemical environments give rise to different chemical shifts. The differences that are observed in an NMR spectrum give rise to NMR spectroscopy's widespread use in chemistry.

Spin-Spin Splitting

The origin of the splitting observed in an NMR spectrum is the influence of the interaction of adjacent NMR active nuclei. The magnitude of this interaction is denoted by a spin-spin coupling constant, J_{AB}.[2] For example, the resonance of a proton on one carbon will be split through interactions of protons on an adjacent carbon ($CHCl_2$-CH_2-Cl). The proton in $CHCl_2$ unit will be split by the two protons on the CH_2 group, forming a triplet with relative intensities of 1:2:1 (Figure 2).[3] The explanation lies in the fact that the two CH_2 protons can form any of three orientations with respect to the applied magnetic field: a) both aligned with the field, b) one with the field and the other against,

and c) both against the field. Since b can happen in two different ways because there are two individual nuclei as observed in the figure below, the intensities of the peaks are 1:2:1.[3]

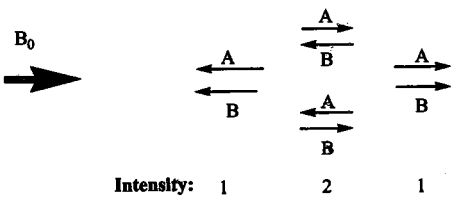

Figure 2. The relative intensities of the peaks within a triplet are due to the probability of having each possible orientation with respect to the external magnetic field.

The difference in energy that it takes to bring each one of the above three scenarios into resonance is slightly different. Therefore, the signal that is received by the instrument is split into three peaks and thus giving rise to spin-spin splitting. The general rule to NMR is that the multiplicity is $n + 1$ where n is the number of adjacent protons.

The ^1H NMR spectrum of the alkyl portion of ethyl benzene is shown in Figure 3. The terminal CH_3 group is a triplet in the spectrum while the CH_2 is as a quartet. The multiplicity of the resonances on the adjacent NMR active nuclei is present due to factors as described above. The extensive splitting which is observed in the spectrum if Figure 3 is due to the fact that spins of the protons on the aromatic ring interact over long molecular distances. This causes the extra splitting of the peaks of the ethyl portion of the ethylbenzene molecule into the "triplet of doublets" and the "quartet of doublets".

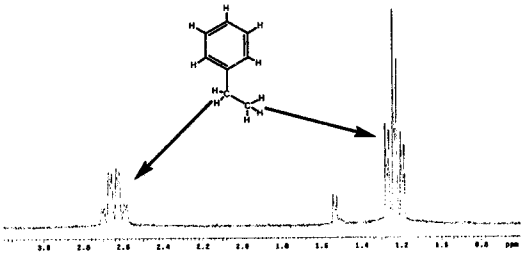

Figure 3. The enlarged ethyl portion of the ^{1}H spectrum of ethylbenzene showing the effect of spin-spin splitting on adjacent NMR active nuclei and those that arise from long range interactions.

Thus far spin-spin splitting for hydrogen nuclei using ^{1}H NMR spectroscopy has been described. However, the phenomenon of spin-spin splitting is not limited to this application. Any nucleus that is NMR active will split the signal of adjacent NMR active nuclei. The splitting is observed readily in ^{1}H NMR due to the natural abundance (over 99 %) of ^{1}H hydrogen. The abundance of other NMR active nuclei can be much less. For example, in ^{13}C NMR spectroscopy, the ^{13}C isotope of carbon is only ~ 1 % abundant in nature. Therefore the likelihood of having two ^{13}C nuclei adjacent to each other, and thus observing spin-spin splitting, is about 1 in 10,000. In order to be able to observe spin-spin splitting in ^{13}C NMR spectroscopy (run decoupled to ^{1}H interactions), the sample must be synthesized with isotopically enriched ^{13}C nuclei. In this case, the sample would show spin-spin splitting much like that observed in a proton spectrum.

NMR Spectroscopy in Organic Chemistry
➢ Drug Design and Development

As Nuclear Magnetic Resonance technology developed, it found wide use in the field of organic chemistry before taking root in other disciplines. The major role of NMR in organic chemistry is to characterize the products of organic syntheses. Typical organic NMR spectra look like those shown above for ethylbenzene, however, as the molecules become more complex, the NMR spectra follow suit giving valuable information about a molecule's identity. One of the most active areas of organic chemistry today is the field of drug research and development. As with other areas of organic chemistry, NMR has proven to be a very powerful tool in characterizing and researching many of the drugs that are on the market today.

With the amount of work currently being done in the pharmaceutical field, the development of NMR applications specific to this field have become a major trend. Once such technological advance utilizes NMR to help elucidate the structures of drug receptors with and without the drug present. These studies can show how the drug and its receptor interact and can lead to new drug discoveries.[4] Although most drugs are not discovered in this way, the NMR and x-ray crystallographic methods now available to image the target drug receptor and subsequently design a drug to fit into the active site of that receptor are making this a more plausible route.[4]

As stated above, one application of NMR spectroscopy to drug development is to determine how the drug interacts with its receptor. When a drug comes into contact with its receptor, perturbations in the chemical shift of both the drug and the receptor signal usually exist. The NMR signals from the two change as there are changes taking place in both the receptor and the drug molecule. These changes show up as shifted resonances in

the NMR spectrum. In an ideal situation, the spectroscopic properties of the receptor and drug are known such that any new resonances that show up on the spectrum are indicative of a bound drug.[4]

Another method of using NMR for drug development is first finding a lead compound from a large library and then second, modifying it to try and make the receptor interactions more specific. This large scale screening can be a faster method of finding a potential drug than rational design as described above. The large libraries are screened using a bio-assay which is suitable for the desired receptor interaction. Then, through radioactive isotope labeling studies, the bio-assay is used to detect which compounds in the library show interaction with the target. The advantage to using NMR techniques in place of these traditional bio-assays is that NMR can detect weaker binding interactions and are therefore more sensitive.[4,5]

From the above example, it can be seen that within the field of organic chemistry and especially drug development, NMR finds great use in the characterization of novel molecules.

NMR spectroscopy in Inorganic Chemistry

Although NMR had its roots in organic chemistry, the same principles provide insight into novel syntheses in inorganic chemistry as well. Unlike organic chemistry which relies heavily on ^{1}H and ^{13}C NMR spectroscopy, inorganic chemistry utilizes other spin-active nuclei as well. For example, ^{59}Co NMR spectroscopy is very sensitive and can detect very small changes in cobalt containing complexes. This property is shown very clearly in work done by Braunstein et. al.[6] In this research, the group synthesized

both $RuCo_3$ and $FeCo_3$ carbonyl cluster complexes. Traditionally, the orientation of the carbonyls (or the other ligands) is confirmed using x-ray crystallography. However, they have shown that very small changes in the ligand frame, such as the replacement of one ligand with a phosphine or amine ligand can cause evident changes in the ^{59}Co NMR spectrum. Figure 4 shows the progress of a ligand exchange reaction using ^{59}Co NMR. The only difference in complexes **1** and **2** is the replacement of one CO ligand with an NMe_3. The differences in ^{59}Co spectra however, are drastic. As observed in Figure 4, the change of one ligand results in a shift of 84 ppm in one cobalt resonance from -2615 ppm to –2531 ppm. Additionally, a new peak arises at – 783 ppm which corresponds to the cobalt with the amine attached to it. It is also observed that although complex **1** does not entirely convert to **2**, some does and then it is converted back to **1** after the three hour experiment.

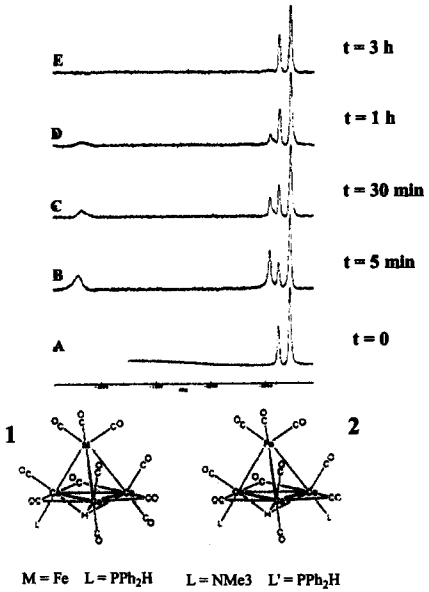

Figure 4. A series of ^{59}Co NMR spectra demonstrates the ability to monitor the interconversion of complex **1** to complex **2** and then back to complex **1**. Spectrum A is a pure spectrum of **1** and t=0, B is at t = 5 min, C is at t = 30 min, D is at t = 1 h, and E is at t = 3h. The series of NMRs shows the rapid formation and disappearance of **2** over time.

As seen above, other nuclei besides ^{1}H and ^{13}C yield valuable structural information. The wide variety of possible nuclei gives rise to a vast range of uses for NMR spectroscopy.

Uses of NMR spectroscopy Outside of Chemistry

The theory behind NMR spectroscopy has also found use in other fields such as clinical diagnosis. The transition between the chemical and clinical came with the ability to *image* a sample as opposed to detecting a spectrum on a page. Magnetic Resonance Imaging (MRI) abides by the basic NMR principles, however, the imaging techniques used are able to exploit differences in the tissues through differences in the chemical environments of protons in water in the tissues. These differences are either related to the relaxation times of the protons or to the differences in the proton density in the tissue. Nevertheless, MRI imaging is an extension of classical NMR spectroscopy and has provided clinicians with tools for a more accurate diagnoses.[7]

Bio-Inorganic Chemistry:

- **The World of Model Complexes**

A sub-discipline of inorganic chemistry is the field of bio-inorganic chemistry. This field is dedicated to the study of biologically active compounds which contain a metal center. One has to go no further than the human body to find many compounds that contain metal centers. Examples include the oxygen carrier that humans have in their blood, hemoglobin, which contains an iron center bound by a porphyrin ring. Vitamin B-12, which is essential to humans and catalyzes many reactions within the body is a cobalt based vitamin. Ongoing efforts to understand metals in biological settings include modeling the active sites of enzymes. The goal of these studies is to isolate and characterize complexes which mimic the reactive sites of enzymes in order to elucidate the mechanism of action of the naturally occurring enzyme. These model complexes can

then be used to study the reactivity and properties of the enzyme in order to gain insight into how these bio-molecules function.

One example of a sought after class of enzymes are those that contain an iron-sulfur complex.[8] The clusters in these enzymes are involved in catalyzing redox reactions, most often being one electron transfers. The enzymes work by reducing Fe(III) to Fe(II) within the cluster. One property that makes this cluster suitable for redox reactions is that the orbitals of the atoms in the cluster overlap such that the change in electron density accumulated or lost by the complex is delocalized over all atoms in the cluster.[8]

In current work by Boyke et. al.,[9] the active site of a series of Fe-only hydrogenases, which are iron-sulfur cluster enzymes, are being modeled. These enzymes find natural use in oxidation reactions as would be expected based on the function of iron-sulfur clusters. The structures of the naturally occurring active sites for these complexes are shown below in Figure 5.

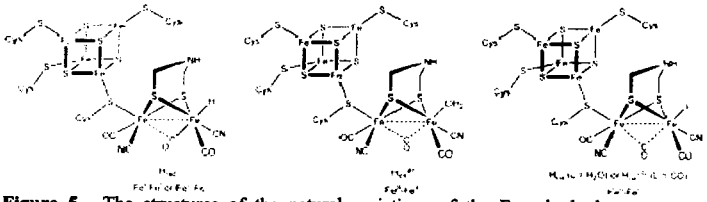

Figure 5. The structures of the natural variations of the Fe-only hydrogenases as published by Boyke et. al.[10]

The group synthesized a set of model complexes of the two Fe subunit of the Fe-only hydrogenases and used ^{31}P NMR characterize them. The model complexes that the group

synthesized (Figure 6) contained a phosphine group that the naturally occurring enzyme does not, allowing the use of ^{31}P NMR in characterization. They mimicked only the two iron cluster as observed above, and they used time dependant ^{31}P NMR (another NMR active nucleus) to monitor a change that they observed in their synthesis. Below is the NMR spectra that the group used to monitor the interconversion. The proposed conversion from the first complex (denoted by a asterisk) to the intermediate (denoted by a solid triangle) and subsequently from intermediate to the final product (denoted by a star) was followed by time dependant ^{31}P NMR as shown in Figure 7.

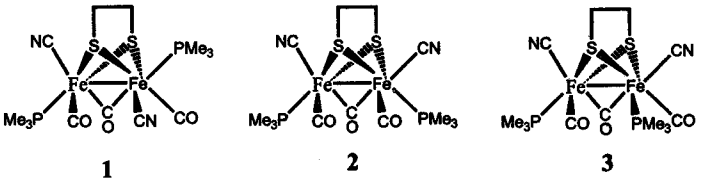

Figure 6. The three model complexes are shown that are characterized using time dependant ^{31}P NMR (Figure 7).

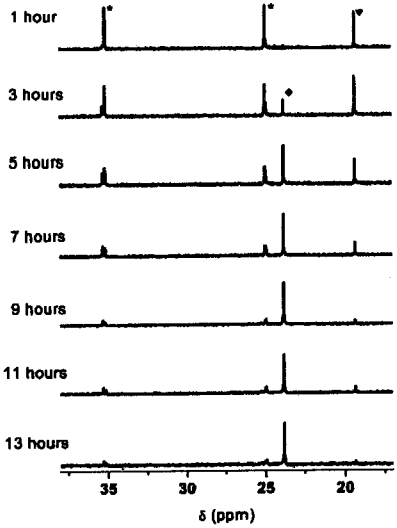

Figure 7. Time-dependant 500 MHz ^{31}P spectra of the model complexes **1**, **2**, and **3** at 60°C. * Indicates signals the starting compound, **1**; ▼ denotes intermediate isomer, **2**; ♦ represents signal for final product, **3**. The gradual disappearance of starting material is accompanied by the appearance of an intermediate at 19.7 ppm.

There are two classes of bio-molecules that contain iron: those that contain a heme and those that do not. Some of the most commonly known biologically relevant iron containing molecules are hemoglobin and other heme-containing proteins. There has, however, been extensive work on non-heme containing complexes by Kurahashi et. al. which was focused on the synthesis of a functioning model complex for the naturally occurring active site which has two histidine and two tyrosine donors forming the ligand frame.[11] These molecules have natural redox activity and an open coordination site for water or hydroxide coordination.[10] Kurahashi et. al. synthesized an Fe-salen based model

complex which mimics the environment of the naturally occurring enzyme. The five coordinate model complex has an open coordination site for exogenous ligands to bind. The structure of the model complex of the non-heme protocatechuate 3,4-dioxygenase enzyme is shown in Figure 8.

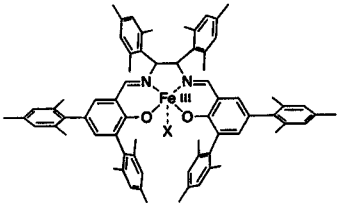

Figure 8. Structure of a model complex of protocatechuate 3,4-dioxygenase.[11]

^{13}C NMR spectroscopy Applications to Bio-Inorganic Cyanide Related Work

The work that we have done involves the integration of the cyanide ligand into the ligand environment of the complex, therefore, it is interesting to note work that has been done to date in the related field of Bio-Inorganic chemistry which involves the cyanide ligand. Cyanide is a known toxic chemical which blocks the elec· on transport chain in the body and thus does not allow for ATP to be made, resulting in fatality. It has been used in the past as a method of committing suicide or poisoning, in addition to finding common applications in rat poisons. Despite these harmful characteristics, there has been extensive work done in different areas of bio-inorganic chemistry with metal-cyanide complexes. For example, Fujii et. al.[11] reported a study on the use of an axial cyanide ligand to determine the identity and properties of the proximal ligand in heme-containing

proteins.[12] Heme-containing proteins have an octahedral active site metal with four of the coordination sites in the basal plane provided by a heme ring. The CN^- is bound to one of the axial sites while the site trans to the CN^- is occupied by a histidine residue which is hydrogen bound in a slightly different chemical environment. The four enzymes that were studied were human hemoglobin and horse heart cytochrome c which have a histidine hydrogen bound to a keytone, sperum whale myoglobin with its histidine hydrogen bound to an alcohol, and Horseradish peroxidase with its histidine hydrogen bound to an acid. When ^{13}C NMR spectroscopy was performed on these complexes, the very small change in the proximal ligand environments gives rise to a noticeable change in the NMR spectrum. The fact that the group was able to distinguish between such small differences shows the extreme sensitivity of NMR spectroscopy and its applications to characterization. Figure 9 shows the complexes that the group studied and the resulting ^{13}C NMR spectra.

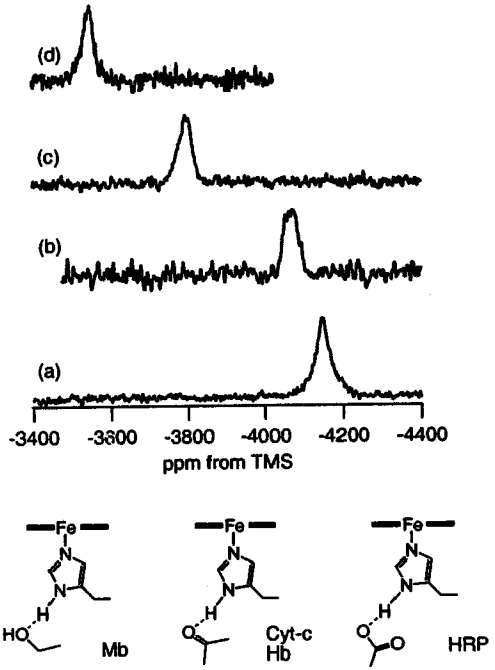

Figure 9. The structures of the environment of the proximal ligand are shown on the bottom and are sperum whale myoglobin (Mb), human hemoglobin (Hb), horse heart cytochrome c (Cyt-c), and horseradish peroxidase (HRP). Above are the ^{13}C NMR spectra showing the cyanide resonances for the respective proteins: (a) Sperum whale myoglobin (b) Human hemoglobin (c) Horse heart cytochrome *c* (d) Horseradish peroxidase.

Current Research

Although much work has been done using NMR spectroscopy in all fields of chemistry, very little has been done exploring the effect that the metal center has on the ^{13}C resonances and the ability of coupling to take place through a metal center. In fact, to date, no metal complexes have been reported which exhibit ^{13}C / ^{13}C coupling through the metal center.

The study of spectroscopic techniques related to biologically relevant metal complexes could provide new methods of analysis for such species. As such, studies that further identify new spectroscopic techniques in the field are of value. The research presented here explores the spectroscopic properties of metal complexes containing more than one labeled ^{13}C carbon atoms.

When studying dicyano complexes, there are two different ways that the two cyanide ligands can coordinate to the metal center. If the two cyanides coordinate adjacent to each other (90° apart), than they termed "cis", if they are oriented 180° from each other they are "trans" (Figure 10).

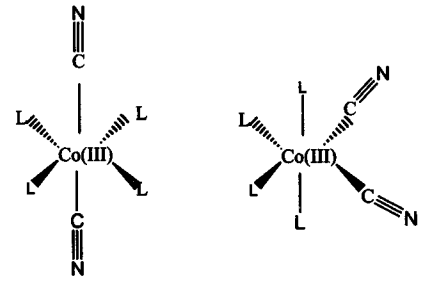

Figure 10. A general view of the cis- and trans- arrangements of the cyanide ligands, where L represents a general Lewis base.

If the ligand frames for two complexes are asymmetric in the dicyano complexes, there is expected to be a different ^{13}CN resonance for each cyanide in each complex. The possible spectroscopic differences between the cis- and trans- configuration could yield insight into new conformational analysis techniques for characterization of transition metal complexes. The labeling studies utilize ^{13}CN which results in a) signal enhancement, and b) observable spin-spin splitting interactions between the cyanide ligands. To date, there has been no observation of through metal splitting and the factors that affect the coupling.

EXPERIMENTAL

All solvents used were purchased dried. The triethylamine used was distilled before use.

$Et_4N^{13}CN$.

A batch of 1 g (20.41 mmol) $Na^{13}CN$ was added to a 250 mL round bottom flask and 100 mL of dry methanol. To this slurry, 3.38 g (20.41 mmol) of NEt_4Cl was added and the resulting slurry was stirred for 72 h. White sodium chloride solid was isolated on a Schlenk frit. The solvent was removed from the mother liquor by vacuum and product was isolated in quantitative yield. ^1H NMR spectrum (DMSO, 200 MHz) δ from TMS: 1.1 (m), 3.2 (m) ^{13}C Spectrum (DMSO, 50.28 MHz) δ from TMS: 15, 52.

2,6-pyridinediacid chloride (1).

A batch of 2.5 g (15.0 mmol) of 2,6-pyridinedicarboxylic acid was dissolved in 80 mL $SOCl_2$ in a 250 mL round bottom flask. The white slurry was refluxed 24 h and resulted in a colorless homogeneous solution. The $SOCl_2$ was pulled off via short path distillation resulting in a white solid. The solid was triturated 5 times with 30 mL dry chloroform and dried for 24 h under vacuum. Yield: 2.5 g (82 %). ^1H NMR ($CDCl_3$, 200 MHz) δ from TMS: 8.24 (m). Selected IR Bands (v, cm^{-1}): 1738.03 (v_{CO}).

Tritylated Aminothiophenol (2).

A batch of 15.0 g (57.6 mmol) triphenylmethanol was dissolved in 100 mL trifluoroacetic acid (TFA) in a 250 mL round bottom flask. To this solution was added a solution of 7.21 g (57.6 mmol) 2-aminothiophenol in 10 mL methylene chloride resulting in a yellow

/ brown solution). The solution was stirred 1 h and then the TFA was removed by vacuum distillation. When dry, the yellow solid was added to a saturated solution of sodium bicarbonate and stirred for 1 h. The brown/yellow solid was extracted with 250 mL chloroform, filtered, and the chloroform was pulled off via rotary evaporation. The off white/brown solid was re-crystallized by slurrying the crude powder in methanol and cooling to 0 °C for 24 h. This resulted in an off white/brown powder.[12] Yield: 16.5 g (78 %). ^{1}H NMR spectrum ($CDCl_3$, 200 MHz) δ from TMS: 4.83 (s), 6.21 (t), 6.50 (d), 6.75 (d), 7.26 (m). Selected IR Bands (v, cm^{-1}): 3368.24 (ν_{NH}).

PyPS-Try (3).

A batch of 8.141 g (22.9 mmol) **2** was dissolved in 30 mL dry chloroform in a 100 mL beaker. To this, 1.469 mL (19.95 mmol) NEt_3 was added. In a separate 250 mL round bottom flask, 2.058 g (11.4 mmol) **1** was added and dissolved in 40 mL dry chloroform and 1.469 g (19.95 mmol) NEt_3. The solution of **2** was added drop wise to the solution of **1** forming a yellow/brown solution and a vacuum applied after each 2-3 mL addition of **1** to remove a white gas that formed above solution. A white/brown precipitate began to form after about 15 min and the reaction was left to stir over 2 days. The white/brown precipitate that was formed was isolated on a Büchner funnel and washed with 50 mL of ice cold methanol and then dried on high vacuum.[12] Yield: 5.745 g (56 %). ^{1}H NMR spectrum ($CDCl_3$, 200 MHz) δ from TMS: 6.76 (t), 6.98 (t), 7.14 (d), 7.54 (d), 7.616 (t), 8.18 (d), 8.32 (d), 8.61 (d), 10.54 (s, amide NH). Selected IR Bands (v, cm^{-1}): 1673.94 (ν_{CO})

$PyPSH_4$ (4).

1.0 g (1.112 mmol) **3** was dissolved in 25 mL TFA in a 50 mL Schlenk flask resulting in a bright yellow-orange solution. To this, a batch of 0.517 g (4.449 mmol) triethylsilane was added and nitrogen was backfilled into the flask, forming a bright canary yellow solution with a thick white precipitate. The precipitate was removed using a Schlenk frit and the TFA was removed in vaccuo to give a white solid powder. This powder was triturated three times with 20 mL chloroform. The third 20 mL portion of chloroform was added about 10 mL of Et_2O until a solid white powder precipitated out of solution.[12] Yield: 0.380 g (90 %). ^1H NMR spectrum ($CDCl_3$, 200 MHz) δ from TMS: 3.39 (s, 2H, SH), 7.12 (t, 2H), 7.41 (t, 2H), 7.58 (d, 2H), 8.19 (t, 1H), 8.37 (d, 2H), 8.57 (d, 2H), 10.493 (s, 2H, NH). Selected IR Bands (v, cm^{-1}): 1679.38 (ν_{CO})

$(Et_4N)_2[Co_2(PyPS)_2]$ (5).

A batch of 300 mg (0.791 mmol) of **4** was dissolved in 20 mL DMF in a 50 mL Schlenk flask yielding a brown-orange solution. The flask was backfilled with nitrogen and a batch of 0.788 g (3.283 mmol) NaH was added. The slurry was further degassed and allowed to react completely. After 10 min, 0.198 g (0.791 mmol) of $[Co(NH_3)_5Cl]Cl_2$ was added and the solution was heated at 70 °C for 1.5 h until the solution turned a deep red/brown. The heat was removed from the solution and 0.275 g (1.66 mmol) $(Et_4N)Cl$ was added. The solution was stirred for 6 h and then the DMF was removed in vacuo. The black residue was redissolved in 45 mL of acetonitrile and vigorously stirred. The solution was then filtered and the volume reduced to 20 mL. The solution was then kept at 0 °C for 24 h. The deep black crystals were collected and dried

in vacuo.[13] Yield: 0.372 g (41 %) ^{1}H NMR spectrum (DMSO, 200 MHz) δ from TMS: 1.34 (m), 2.076 (s), 3.155 (m), 5.144 (d), 6.283 (t), 6.586 (t), 6.782 (t), 6.873 (m), 7.084 (t), 7.725 (m), 8.119 (m), 8.473 (d). ^{13}C Spectrum (DMSO, 50.28 MHz) δ from TMS: 8.7, 46.0, 76.6, 77.2, 77.9, 119.2, 122.3, 123.7, 125.4, 126.0, 129.2, 134.8, 137.9, 139.9, 149.2, 161.4. Selected IR Bands (ν, cm^{-1}): 1617.70 (ν_{CO})

[Co_2(PyPS(SMe))$_2$] (6).

A batch of 218 mg (0.190 mmol) of **5** was dissolved in 15 mL of CH_3CN in a 50 mL round bottom flask. Next, 480 μL CH_3I was added and the reaction was stirred for 2 h and then left to sit without stirring for an additional 1 h. A black microcrystalline solid was isolated by gravity filtration, washed with 5 mL CH_3CN and was air dried.[14] Yield: 95 mg (56 %). ^{1}H NMR spectrum (DMSO, 200 MHz) δ from TMS: 1.25 (s, SMe), 5.47 (d), 6.54 (t), 7.18 (m), 7.54 (m), 8.09 (d), 8.17 (d) 8.47 (t), 8.67 (d). Selected IR Bands (ν, cm^{-1}): 1617.70 (ν_{CO})

(Et_4N)$_2$[Co(PyPS(SMe))(CN)$_2$ (7)

A batch of 94 mg (0.104 mmol) of **6** was suspended in 15 mL CH_3CN in a 25 mL round bottom flask. Next, a batch of 94 mg (0.561 mmol) of NEt_4CN was added in 1 mL (7.695 mmol) CH_3CN and the slurry was stirred for 2 h. The resultant dark red-orange homogeneous solution was then gravity filtered. Crystalline product, **7**, was obtained by diffusing Et_2O into the CH_3CN solution. The red-orange crystals were isolated and dried in vacuo.[14] Note: Isotopically labeled $Et_4{}^{13}CN$ was used to make the ^{13}C labeled derivative, **8**. Yield: 70 mg (55 %) ^{1}H NMR spectrum (DMSO, 200 MHz) δ from TMS:

1.11 (m), 2.23 (s, SMe), 3.14 (q), 6.50 (t), 6.77 (t), 7.15 (m), 7.55 (m), 7.37 (m), 8.11 (t), 8.69 (m). ^{13}C Spectrum of the ^{12}CN complex (DMSO, 125.8 MHz): 17.5, 51.3, 119.3, 121.3, 121.4, 121.9, 122.0, 122.7, 124.4, 127.3, 127.7, 135.4, 137.3, 137.5 (CN), 140.7 (CN), 147.4, 148.7, 149.5, 155.0, 157.6, 162.7, 164.4. ^{13}C Spectrum of the ^{13}CN complex (DMSO, 50.3 MHz): 17.5, 51.3, 119.3, 121.3, 121.4, 122.01, 122.09, 122.8, 124.5, 127.4, 127.8, 135.5, 137.4, 137.98 (d, CN), 141.3 (d, CN), 147.4, 148.7, 149.5, 155.0, 157.6, 162.7, 164.4. Selected IR Bands (ν, cm^{-1}): 2114.42 (ν_{CN}), 1611.10 (ν_{CO})

$(Et_4N)_2[Co(PyPS(SMe))(^{12}CN)(^{13}CN)_2$ (9)

A batch of 94 mg (0.104 mmol) of **6** was dissolved in 20 mL dry acetonitrile in a 50 mL round bottom flask. Added to this was a solution of 47 mg (302 mmol) of $NEt_4{}^{13}CN$ in 1 mL CH_3CN. This reaction was stirred for 1 h and then a solution of 47 mg (302 mmol) $NEt_4{}^{12}CN$ in 1 mL CH_3CN was added to the reaction. The reaction was then stirred for 1 additional hour and then the dark red solution was gravity filtered to remove un-reacted starting material. Crystalline product was obtained by diffusing Et_2O into the CH_3CN solution. Yield: 72 mg (56 %) ^1H NMR spectrum (DMSO, 200 MHz) δ from TMS: 1.11 (m), 2.23 (s, SMe), 3.14 (q), 6.50 (t), 6.77 (t), 7.15 (m), 7.55 (m), 7.37 (m), 8.11 (t), 8.69 (m). ^{13}C Spectrum (DMSO, 50.3 MHz): 17.5, 51.3, 119.3, 121.3, 121.4, 122.01, 122.09, 122.8, 124.5, 127.4, 127.8, 135.5, 137.4, 137.6 (s, ^{12}CN / ^{13}CN complex) 137.98 (d, ^{13}CN / ^{13}CN), 140.8 (s, ^{12}CN / ^{13}CN complex), 141.3 (d, ^{13}CN / ^{13}CN), 147.4, 148.7, 149.5, 155.0, 157.6, 162.7, 164.4. Selected IR Bands (ν, cm^{-1}): 2106.11 (ν_{CN}), 1612.34 (ν_{CO}).

RESULTS AND DISCUSSION

Syntheses

➢ $PyPSH_4$ Ligand Synthesis

The first step in the synthesis of the ligand was, 1) the conversion of 2,6-pyridinedicarboxylic acid into the diacid chloride and 2) the protection of the thiol in the 2-aminothiophenol molecule. These two steps can be found in the first two steps of Scheme 1.

Starting from the beginning with the synthesis of the diacid chloride, the most important part of this synthesis is to make sure that it is void of any excess thionyl chloride. First, it is important that the reaction be refluxed for ~24 h in order to react all 2,6-pyridinedicarboxylic acid to the diacid chloride. It is of great importance upon the work-up of the acid chloride that all residual thionyl chloride is removed. This is accomplished by thorough trituration of the product at least three to five times with chloroform followed by drying it overnight under high vacuum. The diacid is normally white in color not a shade of pink. If there is residual $SOCl_2$ in the product, the PyPS-Try ligand synthesis will have very low yield. Instead of the triethylamine reacting with the amine proton on the trityl-protected 2-aminothiophenol, it will instead be used up by the excess $SOCl_2$.

Step two in the reaction is to make the trityl-protected 2-aminothiophenol. The trityl protecting group is added to the 2-aminothiophenol to prevent any unwanted reaction of the thiol group during ligand synthesis. The first part of this synthesis is the addition of trityl and 2-aminothiophenol in TFA. In order to make clean protected thiol that is not contaminated with residual trifluoroacetic acid (TFA), care must be taken to remove all of the TFA. This is done by carefully washing the product with a saturated

solution of sodium bicarbonate. The crude protected thiol does not dissolve in the sodium bicarbonate solution and therefore in order to maximize yield of clean protected thiol, the slurry must be continuously stirred very well. Also, the solution must remain saturated with sodium bicarbonate and it is advantageous to add excess sodium bicarbonate to the solution. After the wash is complete, it is important to note that there should be no yellow color to the methanol or in the solid, as this is an indication of excess TFA. The re-crystallization methanol should be clear, light grey/brown in color with the solid being the same color.

Step three combines the diacid chloride and the protected thiol to make the pentadentate protected ligand, PyPS-Try. This reaction requires triethylamine to remove one of the amine protons on the protected 2-aminothiophenol so that it can react with the acid chloride. One of the most important parts of this synthesis in order to increase the yield to the highest extent possible is to have freshly distilled triethylamine. The use of fresh triethylamine will increase the effectiveness of the base and therefore will cause more of the starting material to be converted to product.

It is also important to note that the method of de-protection of the trityl is through the addition of acid. Since the synthesis of the ligand generates two equivalents of HCl, care must be taken to evacuate the reaction vessel after each two to three pipets of protected thiol is added to the acid chloride. If not evacuated, the HCl can deprotect the trityl and cause the intramolecular formation of disulfides in the ligand as the two thiol groups will react together.

After the addition of the NEt_3, the solution should turn to a light brown / beige color with a white precipitate. The precipitate should begin to form less than 10 min after

the addition of the protected thiol and most of the precipitate will generally be present within 24 hours after the start of the reaction although the reaction is generally stirred for ~ 48 h. The bright white color does not become fully apparent until the solid precipitate is collected on a Büchner funnel and is washed with ice cold methanol.

The ^{1}H NMR of PyPS-Try is shown in Figure 11. The peak at 10.54 ppm is identified as the carboxamide nitrogen (CO-NH) and identifies that the ligand has been made from the two starting materials. Finally, just below seven, are two disproportionately large peaks in the aromatic region, which are consistent with the triphenylmethanol (trityl) protecting group.

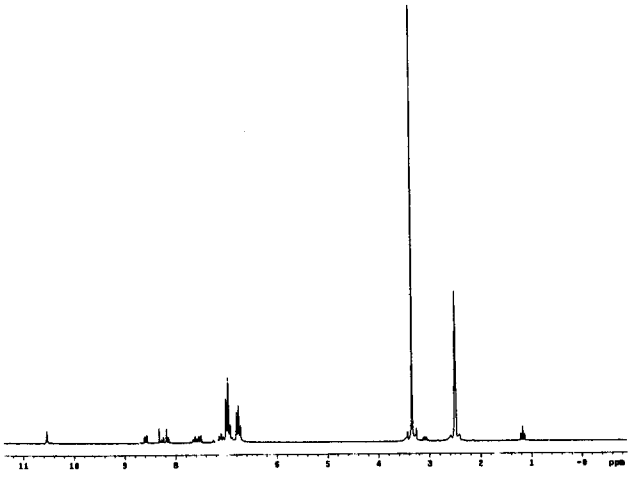

Figure 11. The ^{1}H NMR spectrum of PyPS-Trityl in DMSO acquired on a 200 MHz NMR instrument.

The final step in the synthesis is hard because once the trityl is removed and the thiols are exposed, care must be taken to keep the reaction from air and water to the greatest extent possible, as the formation of disulfides are again an issue. This is also the most important step in the synthesis of the ligand as it renders the final ligand pentadentate.

The isolation of the $PyPSH_4$ is carried out in two steps: The first is the removal of the trityl group, and the second is the isolation of the $PyPSH_4$. In the first step of the synthesis, triethylsilane is added to the ligand dissolved in degassed TFA. Upon addition, an immediate thick white precipitate forms. The precipitate is removed from the de-protected ligand using a Schlenk frit. The TFA is then removed using high vacuum. It is of prime importance that the Schlenk frit be clean and dry so that no water or contaminants are introduced into the mother liquor which contains the product ligand. This can be accomplished by drying the frit in the oven and then removing it and capping both ends with air-tight seals until it is cooled to room temperature.

Once all of the TFA is removed, the resulting light beige solid must be dried and triturated at least three times with chloroform to remove any residual TFA. During the last trituration, Et_2O is added to the chloroform solution and the ligand precipitates out as a white solid. The ligand is collected on a Schlenk frit and dried overnight before use.

Upon de-protection, the ^1H NMR in chloroform reveals a new peak at 3.39 ppm which is the –SH peak. The other peaks remain in the same places, including the carboxamide resonance at 10.49 ppm.

The fact that there are two carboxamide and thiol protons on each ligand, and these proton resonances integrate to one signifies that the two are chemically equivalent,

and that there is an element of symmetry in the ligand. The full proton NMR spectrum of $PyPSH_4$ is shown in Figure 12.

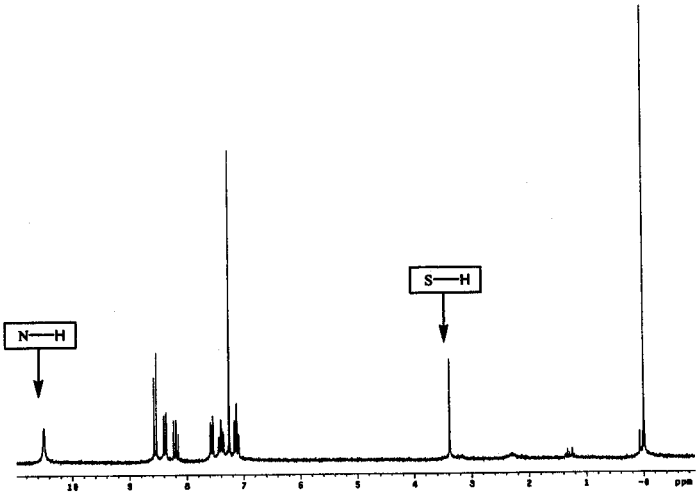

Figure 12. The ^1H NMR spectrum of $PyPSH_4$ in $CDCl_3$ acquired on a 200 MHz NMR instrument.

The synthesis in its entirety is shown in Scheme 1. Once isolated, $PyPSH_4$ can be ligated to the metal center.

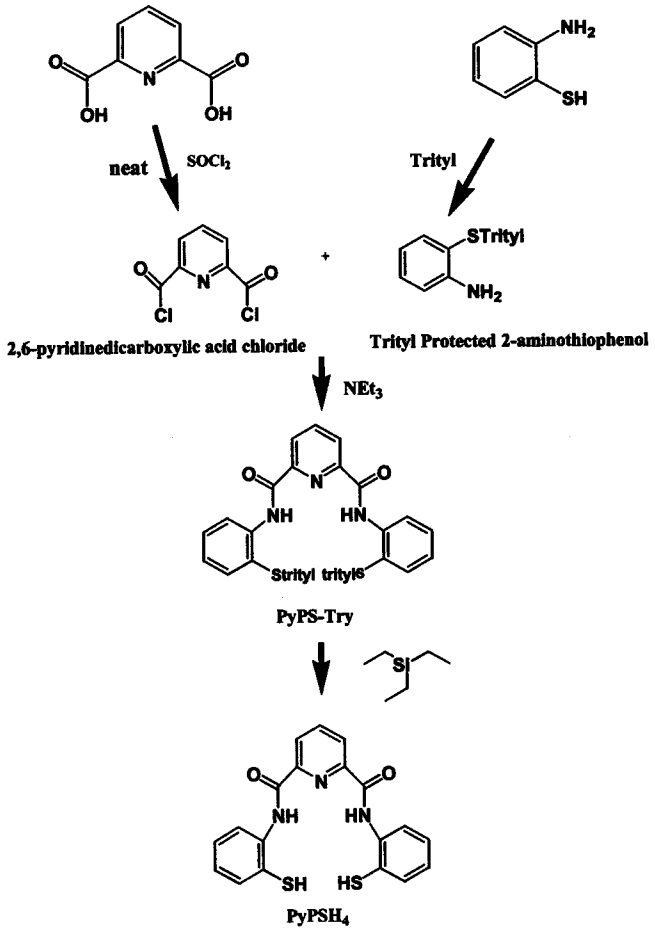

Scheme 1. Synthetic Scheme for $PyPSH_4$ Synthesis.

➢ Synthesis of the Asymmetric Dicyano Complexes

In order for the ligand to bond to the metal center, it must first be deprotonated. The ligand is dissolved in DMF and to this the NaH is added. At this point in the reaction, the solution is a bright red/orange color. Once the solution ceases to evolve gas, the $[Co(NH_3)_5Cl]Cl_2$ is added as a solid. The mixture is then heated to 70 °C for 1.5 h. Heat is applied because the cobalt starting material, $[Co(NH_3)_5Cl]Cl_2$ has a Co^{III} metal center. This cobalt center is d^6, low spin. Complexes with cobalt centers of this type are known as inert due to the arrangement of the electrons in the octahedral complex which maximizes its ligand field stabilization energy. Inert complexes are very un-reactive as compared to complexes that are termed "labile" and readily react. The product does not form a single mononuclear complex but rather a dimeric species is isolated with a 2 : 2 ratio of ligand to cobalt. One of the thiolate sulfur atoms from each $PyPS^{4-}$ ligand bridges the two cobalt metal centers together. The dimerization of this complex can be explained by the fact that the $PyPSH_4$ ligand is pentadentate and d^6, low spin, metal centers preferentially form octahedral complexes which are inherently stable.

The ^1H spectrum of $(Et_4N)_2[Co_2(PyPS)_2]$ is shown in Figure 13. The triplet around 1 ppm, and the quartet just above 3 ppm are a result of the tetraethylammonium counterions. The many resonances in the aromatic region is due to the aromatic protons on the $PyPS^{4-}$ ligands. The clean doublet at 5.2 ppm is indicative of the dimeric species.

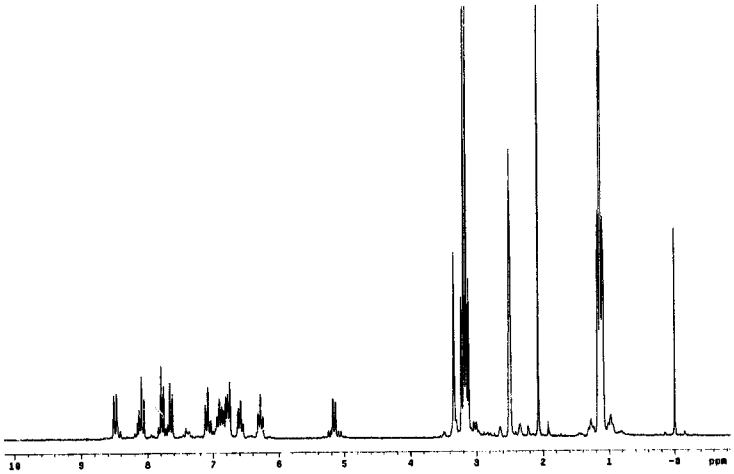

Figure 13. The ^{1}H NMR spectrum of $(Et_4N)_2[Co_2(PyPS)_2]$ in DMSO acquired on a 200 MHz NMR instrument.

The next step in the synthesis is to form the methylated dimer. It is one of the most important steps of the entire synthetic pathway because it imparts asymmetry to the complex. Upon addition of CH_3I to the dimer, only the terminal thiolates react, leaving the bridging thiolates unmodified. The difference in reactivity between the two thiolates is the lack of electron density on the bridging thiolate groups. The bridging thiolate utilizes the majority of its electron density in forming the two Co-μ-S bonds. However, the non-bridging thiolate is only involved in one Co-S bond which leaves an electron pair that acts on the CH_3I in a nucleophilic attack to form a methyl thioether group. A thioether is very similar to a traditional ether except that the oxygen is replaced by a sulfur atom.

Although this specificity in the methylation of the non-bridging thiolate to form the thioether is very useful, care must be taken in order to keep it specific. Because methyl iodide is a very powerful methylating agent, it will eventually begin to methylate the bridging thiolates, causing an over methylation and undesired product. As such, it is crucial to collect the methylated dimer after 2 h.

One of the interesting properties of this reaction is that the starting material is a salt and is soluble in acetonitrile. However, once the thiolates are methylated to the thioether, the product becomes neutral and precipitates out of solution. The ^{1}H NMR spectrum of $[Co_2(PyPS(SMe))_2]$ is shown in Figure 14.

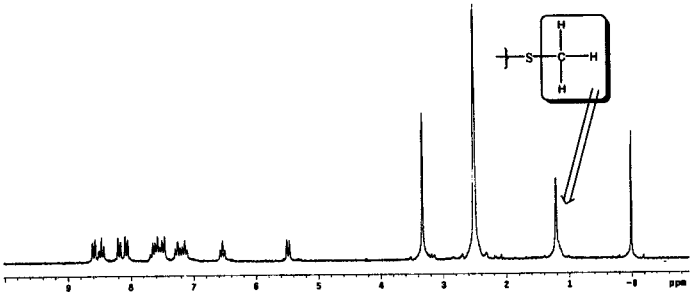

Figure 14. The ^{1}H NMR spectrum of $[Co_2(PyPS(SMe))_2]$ in DMSO collected using a 200 MHz NMR instrument.

The spectrum reveals that the product is very pure as is evident by the flat baseline. The resonance at 5.5 ppm indicates that the species is still dimeric, with the S-CH_3 resonance occurring at 1.2 ppm. Also important to note is the disappearance of the large

tetraethylammonium peaks that were observed because the dimer is no longer negatively charged at 1.1 ppm and 3.2 ppm.

The dicyano complex is then afforded by reacting $(Et_4N)_2[Co_2(PyPS(SMe))_2]$ with 5.8 equivalents of NEt_4CN. The dimer is split into two octahedral dicyano complexes with the four equatorial coordination sites being occupied by the $PyPS^{4-}$ ligand and the axial positions being occupied by the CN^- ligands. The complex undergoes ligand exchange because the CN^- is a stronger ligand than either the thioether or the bridging thiolate. The cyanide ligand is one of the strongest ligands available. The strength is due to the fact that it is a π-accepter ligand. It is available to accept electron density into its empty π* orbital which is symmetry matched with the d-orbitals on the metal center. The π* back donation into the orbital strengthens the overall Co-CN bond. The ^1H NMR of $(Et_4N)_2[Co(PyPS(SMe))(CN)_2]$ is shown in Figure 15 and the synthetic summary is shown in Scheme 2.

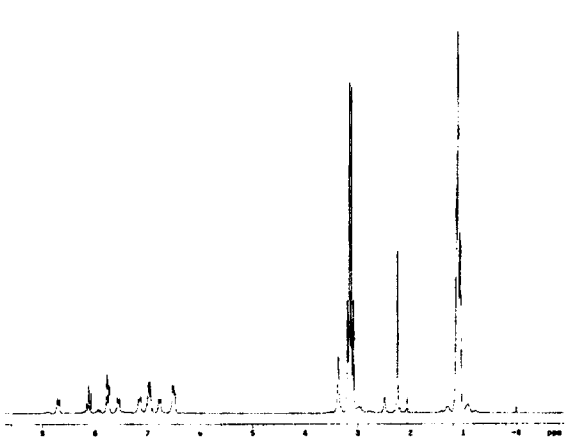

Figure 15. The ^{1}H NMR spectrum of $[Co_2(PyPS(SMe))_2(^{12}CN)_2$ DMSO collected using a 200 MHz NMR instrument.

Scheme 2 shows the entire synthetic scheme for the entire complex synthesis.

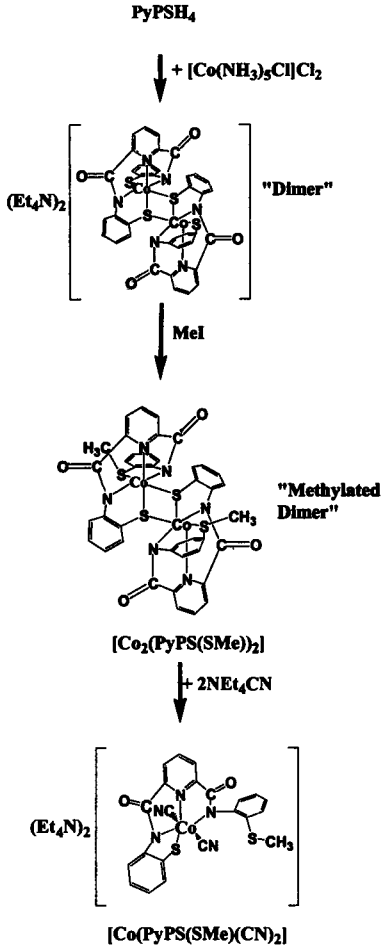

Scheme 2. Synthetic pathway to obtain $[Co_2(PyPS(SMe))_2(^{12}CN)_2]$.

NMR Studies

A pictorial representation of $(Et_4N)_2[Co(PyPS(SMe))(CN)_2]$ is shown in Figure 16. To understand the basis for the asymmetry of the complex, the pendant thioether group must be considered.

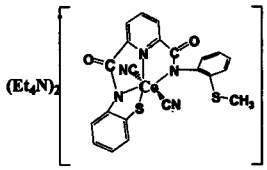

Figure 16. A pictorial representation of $(Et_4N)_2[Co(PyPS(SMe))(CN)_2]$.

Because of the steric crowding, free rotation around the pendant thioether arm does not occur. This gives rise to two separate ^{13}C NMR signals for the cyanide ligands. The ^{13}C NMR spectrum of $(Et_4N)_2[Co(PyPS(SMe))(^{12}CN)_2]$ reveals 22 resonances for 22 different carbon atoms in the complex. This means that every carbon in the complex is in a different chemical environment, and thus, there must be an element of asymmetry in the molecule. The ^{13}C NMR spectrum of unlabeled $(Et_4N)_2[Co(PyPS(SMe))(^{12}CN)_2]$ is shown in Figure 17.

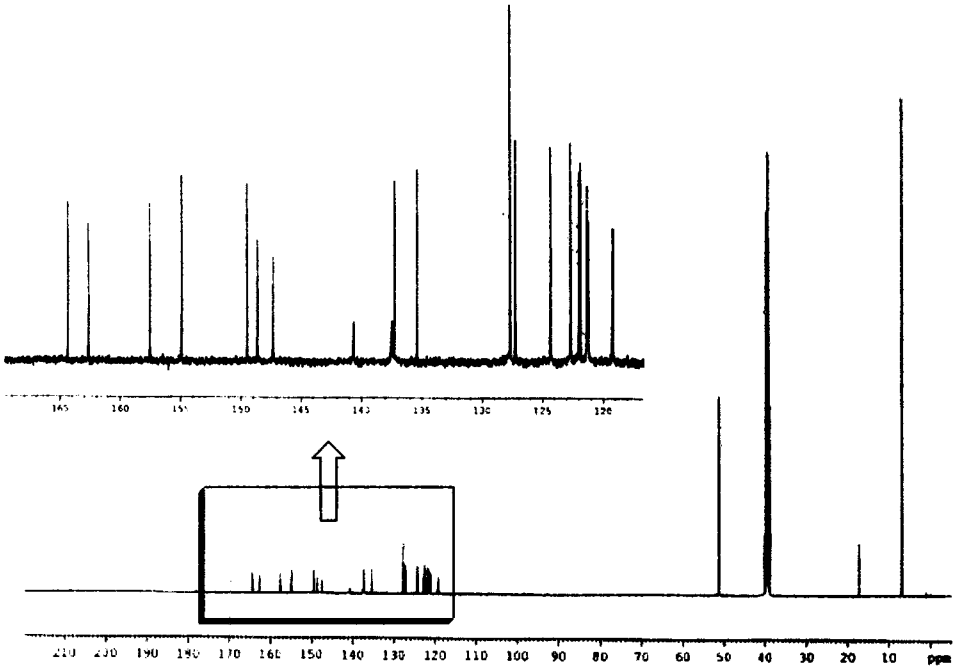

Figure 17. The ^{13}C NMR spectrum of $[(Et_4N)_2[Co(PyPS(SMe))(^{12}CN)_2]$ in DMSO collected using a 500 MHz NMR instrument.

Next, the synthesis was carried out again replacing the ^{12}CN with isotopically labeled ^{13}CN in order to see the possible coupling between the two. Indeed, acquisition of the ^{13}C NMR spectrum of $(Et_4N)_2[Co(PyPS(SMe))(^{13}CN)_2]$ showed a doublet centered around 137.5 ppm and 140.1 ppm. The ^{13}C NMR spectrum of the isotopically labeled $(Et_4N)_2[Co(PyPS(SMe))(^{13}CN)_2$ is shown in Figure 18, with the enlarged cyanide doublets shown in Figure 19.

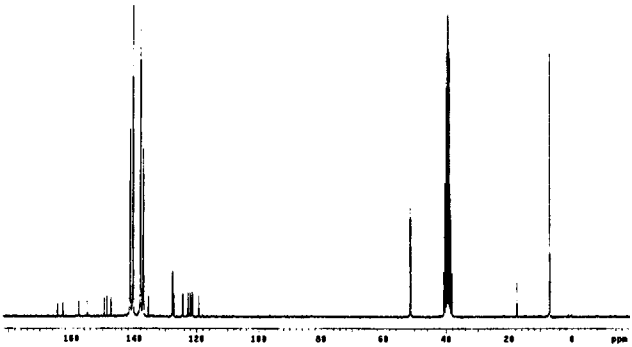

Figure 18. The ^{13}C NMR spectrum of $(Et_4N)_2[Co(PyPS(SMe))(^{13}CN)_2]$ in DMSO collected using a 200 MHz NMR instrument.

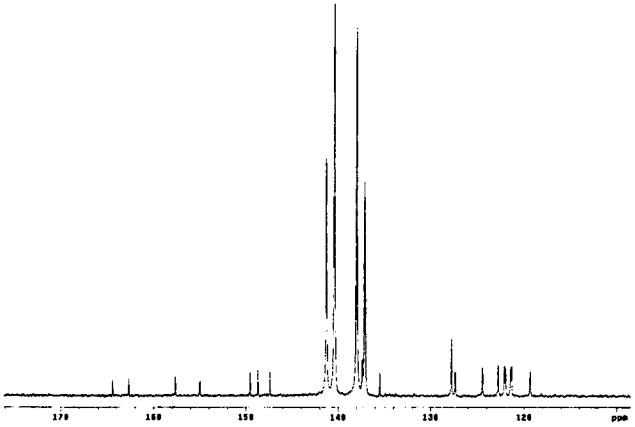

Figure 19. The enlarged cyanide doublets of the ^{13}C NMR spectrum of $(Et_4N)_2[Co(PyPS(SMe))(^{13}CN)_2]$ in DMSO collected using a 200 MHz NMR instrument.

The enlarged region of the ^{13}C NMR in Figure 19 clearly shown the two cyanide resonances are indeed two doublets which center at 137.5 ppm and 140.1 ppm. This through metal splitting has not been previously observed and we report it here for the first time.

In order to further probe that the doublets arise due to the ^{13}CN coupling, we next performed a set of experiments with 50 % ^{13}CN and 50 % ^{12}CN. The thought behind these NMR experiments is that if a 50 % solution of ^{13}C and ^{12}C is added to the methylated dimer, there is a good chance for a ^{12}CN to be located trans in the dicyano complex from a ^{13}CN ligand. Since the only NMR active isotope of carbon is ^{13}C, there should be no through metal spin coupling taking place in this complex and thus, a singlet should be observed for the cyanide. The experiments were carried out three different

ways, varying when the labeled versus the unlabeled CN^- was added to the methylated dimer.

In the first experiment, a 50 : 50 ratio of both ^{12}CN and ^{13}CN added at the same time and made according to the experimental procedure for the dicyano complex. The second experiment was carried out by stirring the ^{13}CN batch (½ of the full amount of cyanide added) for 1 h and then the second half of the cyanide was added as ^{12}CN and it was stirred for the second hour. Finally, in the third experiment, the complex was made by adding the ^{12}CN first, then stirring for an hour and then adding the ^{13}CN after that. The procedures were analogous to the original $(Et_4N)_2[Co(PyPS(SMe))(^{13}CN)_2]$ procedure, except for the addition of the CN^- equivalents at different times.

The enlarged cyanide region of the ^{13}C NMR results of these syntheses are shown in Figure 20. Each of the three synthetic attempts resulted in identical ^{13}C NMR spectra. This suggests that there is no difference in the outcome based on the timing of the addition of cyanide isotopes.

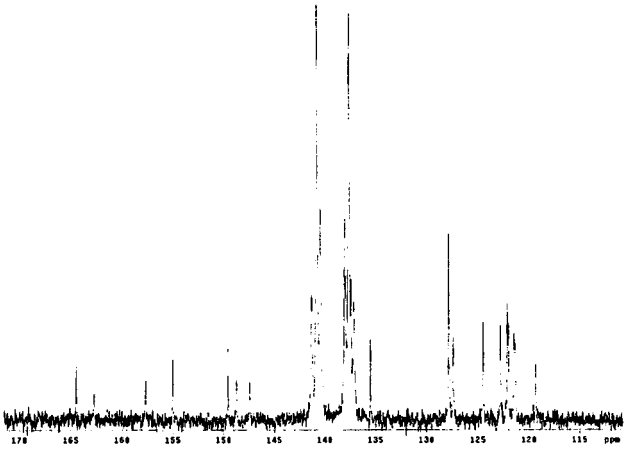

Figure 20. The enlarged cyanide doublets of the ^{13}C NMR spectrum of $(Et_4N)_2[Co(PyPS(SMe))(^{13}CN)(^{12}CN)_2]$ in DMSO collected using a 200 MHz NMR instrument.

Both doublets in the ^{13}CN spectrum have been converted to triplets centered around 140.8 ppm and 137.6 ppm. This splitting can be explained through the following reasoning: The central peak in each triplet is actually a singlet which corresponds to complexes in solution which have one labeled and one unlabeled cyanide ligated. Because the only cyanide that shows up in the NMR is the ^{13}CN, complexes with ^{12}CN and ^{13}CN trans to each other are observed as a singlet. The peaks flanking the singlet peak exhibit the same shift and splitting pattern as the those in the isotopically labeled $(Et_4N)_2[Co(PyPS(SMe))(^{13}CN)_2]$ and are therefore due to the ^{13}CN / ^{13}CN species. It also stands to reason that there are ^{12}CN / ^{12}CN complexes in solution because they have the same likelihood to form as the ^{13}CN / ^{13}CN. These resonances do not show up in an NMR spectrum, however, because ^{12}C is not the NMR active isotope of carbon. As

observed in Figure 20, the peak in the upfield triplet that is between the large middle peak and the right most peak (at 137.4 ppm) is not actually part of the complex, it is another carbon peak in the complex that is unrelated to the cyanides. The cyanide peak was resolved from this peak in the 200 MHz unlabeled dicyano spectrum to a distinct resonance on the 500 MHz instrument.

Upon analysis of the data, it can be conclude that the coupling does indeed arise from $^{13}CN/^{13}CN$ interactions of the cyanide ligands through the metal center. It is also evident that the relative bond strengths of the Co-SCH_3 and the Co-S-Co bonds are similar. Because the two singlets are proportional in size, it suggests that there is no preference for the cyanide to attack one bond versus the other in the methylated dimer.

In order to fully characterize the novel splitting that is observed, temperature dependant studies were performed on the labeled dicyano complex. In order to investigate how the splitting changes with changes in temperature. If the spectrum changes then this suggests that the chemical environment of the cyanide also changes with a change in temperature. The asymmetric dicyano complex contains a pendant thioether arm, which has hindered rotation. The temperature dependence studies also show if the energy barrier to rotation can be overcome at elevated temperatures. The following ^{13}C NMR spectra were obtained (Figure 21).

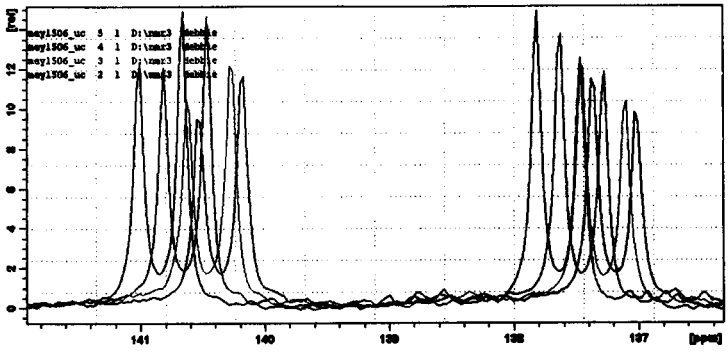

Figure 21. The cyanide region of four $(Et_4N)_2[Co(PyPS(SMe))(^{13}CN)_2]$ 500 MHz NMR spectra. The color of the spectrum corresponds to the temperature at which it was acquired. (blue = 20 °C, red = 30 °C, green = 40 °C and purple = 45 °C).

The trend is for the doublets to remain unmodified, with a slight shift to more upfield resonances at higher temperatures. These studies suggest that the cyanide ligands are still in different chemical environments and that the energy barrier to rotation around the pendant thioether arm is greater than 45 °C. The complete data analysis of the spectra is summarized in Table 1.

Temperature Dependence NMR Studies

		Peak Position (ppm)	Peak Position (ppm)	Separation of Peaks (ppm)
20°C				
	Downfield Doublet	1401.03	140.68	0.35
	Upfield Doublet	137.83	137.47	0.35
30°C				
	Downfield Doublet	140.83	140.48	0.35
	Upfield Doublet	137.65	137.3	0.35
40°C				
	Downfield Doublet	140.64	140.29	0.35
	Upfield Doublet	137.47	137.12	0.35
45°C				
	Downfield Doublet	140.55	140.19	0.36
	Upfield Doublet	137.38	137.04	0.34

	(Table 1 Cont'd)	J_{AB} (Hz)	Doublet Center point (ppm)	Distance Between Doublet Center Points (ppm)
20°C				
	Downfield Doublet	44.02	140.86	3.20
	Upfield Doublet	44.02	137.66	
30°C				
	Downfield Doublet	44.02	140.66	3.18
	Upfield Doublet	44.02	137.48	
40°C				
	Downfield Doublet	44.02	140.47	3.17
	Upfield Doublet	44.02	137.30	
45°C				
	Downfield Doublet	45.28	140.37	3.16
	Upfield Doublet	42.76	137.21	

Table 1. Summarized ^{13}C NMR temperature dependence studies of $(Et_4N)_2[Co(PyPS(SMe))(^{13}CN)_2]$.

The splitting of the doublets is nearly unchanged in each experiment, which means that the cyanide spins interact to the same extent in each experiment. The small change in coupling constant in the 45 °C reading may be due to instrumental error as the coupling constants for all other spectra are exactly the same. The other interesting aspect of these studies is that there is a definite shift of the cyanide resonances to more upfield positions,

accompanied by a very slight decrease in the degree of separation of the two doublets (approximately 0.01 ppm for each 5 °C). If linear, this suggests that the doublets would coalesce after a raise in temperature to 320 °C. This is presumably the temperature at which the pendant arm would have free rotation.

Our findings are further supported by the calculation of the theoretical coupling constant and Fermi coupling constant. The theoretical calculation of the coupling constant (46 Hz) was remarkably close to our experimental values of 42.76 – 45.28 Hz. The large coupling that is observed above is largely due to a large Fermi contact coupling constant for the complex. The large value indicates that there is a great deal of s-character orbital overlap between the two cyanides. Because the cyanides are sp hybrid ligands, there is a great deal of s-character in the bonding orbitals. Secondly, the dz^2 orbital of the metal center is devoid of electron density, thus acting as a wire for the interactions of the sp orbitals of the two trans- cyanide ligands. This gives rise to the large extent of interaction and thus the splitting observed in the NMR.

Future Work

The future of this project revolves around creating more of these types of asymmetric dicyano complexes which show carbon coupling through the metal center. These studies will include starting with an oxidized dimer to make another asymmetric trans- complex as well as the design and synthesis of ligand frames that will direct the CN^- to a cis- conformation.

Appendix A

Table of Contents

A-1 ^{1}H NMR of 2,6-pyridinediacid chloride in DMSO.
A-2 IR of 2,6-pyridinediacid chloride.
A-3 ^{1}H NMR of Trityl Protected 2-aminothio phenol in DMSO.
A-4 IR of Trityl Protected 2-aminothiophenol.
A-5 IR of PyPS-Try.
A-6 ^{13}C NMR of $PyPSH_4$ in $CDCl_3$.
A-7 IR of $PyPSH_4$.
A-8 ^{13}C NMR of $(Et_4N)_2[Co_2(PyPS)_2]$in DMSO.
A-9 IR of $(Et_4N)_2[Co_2(PyPS)_2]$.
A-10 ^{13}C NMR of $[Co_2(PyPS(SMe))_2]$ in DMSO.
A-11 IR of $[Co_2(PyPS(SMe))_2]$.
A-12 IR of $[Co_2(PyPS(SMe))_2(^{12}CN)_2]$.
A-13 ^{1}H NMR of $[Co_2(PyPS(SMe))_2(^{13}CN)_2]$ in DMSO.
A-14 IR of $[Co_2(PyPS(SMe))_2(^{13}CN)_2]$.
A-15 ^{1}H NMR of 50:50 combined addition $[Co_2(PyPS(SMe))_2(^{13}CN)(^{12}CN)]$ in DMSO.
A-16 ^{13}C NMR of 50:50 combined addition $[Co_2(PyPS(SMe))_2(^{13}CN)(^{12}CN)]$ in DMSO.
A-17 IR of 50:50 combined addition $[Co_2(PyPS(SMe))_2(^{13}CN)(^{12}CN)]$.
A-18 ^{1}H NMR of ^{13}CN first $[Co_2(PyPS(SMe))_2(^{13}CN)(^{12}CN)]$ in DMSO.
A-19 ^{13}C NMR of ^{13}CN first $[Co_2(PyPS(SMe))_2(^{13}CN)(^{12}CN)]$ in DMSO.
A-20 IR of ^{13}CN first $[Co_2(PyPS(SMe))_2(^{13}CN)(^{12}CN)]$.
A-21 ^{1}H NMR of ^{12}CN first $[Co_2(PyPS(SMe))_2(^{13}CN)(^{12}CN)]$ in DMSO.
A-22 ^{13}C NMR of ^{12}CN first $[Co_2(PyPS(SMe))_2(^{13}CN)(^{12}CN)]$.
A-23 IR of ^{12}CN first $[Co_2(PyPS(SMe))_2(^{13}CN)(^{12}CN)]$.

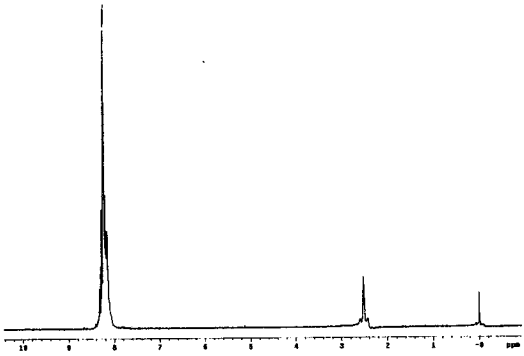

A-1: ^{1}H NMR of 2,6-pyridinediacid chloride in DMSO on a 200 MHz instrument.

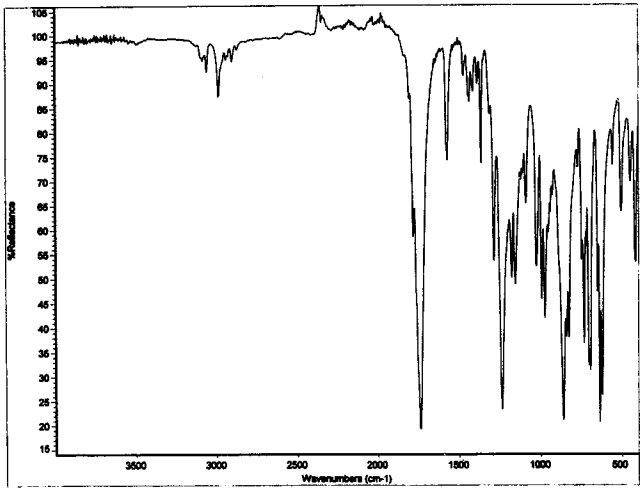

A-2: IR of 2,6-pyridinediacid chloride.

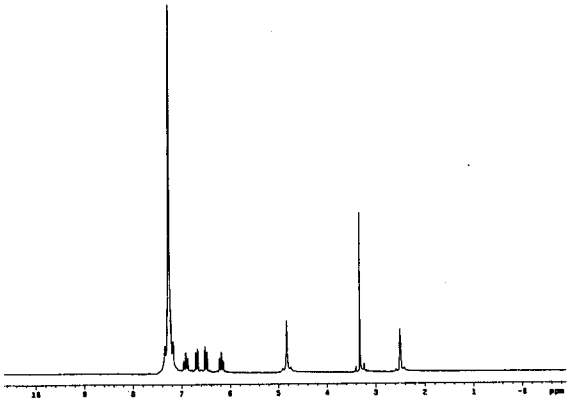

A-3: ^{1}H NMR of Trityl Protected 2-aminothio phenol in DMSO on a 200 MHz instrument.

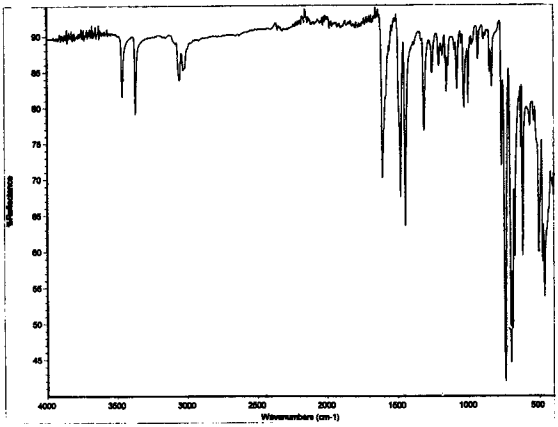

A-4: IR of Trityl Protected 2-aminothiophenol.

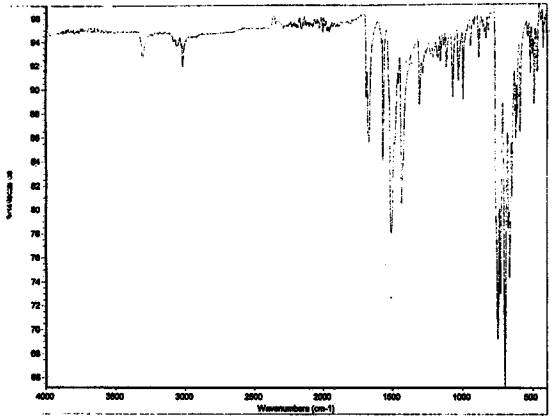

A-5: IR of PyPS-Try.

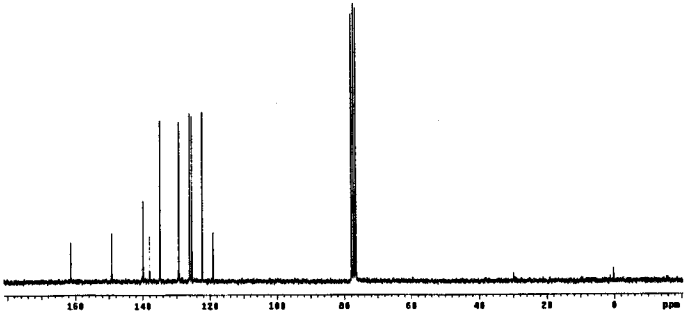

A-6: ^{13}C NMR of $PyPSH_4$ in $CDCl_3$ on a 200 MHz instrument.

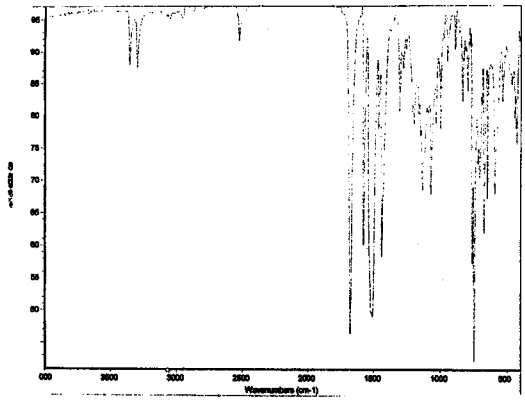

A-7: IR of $PyPSH_4$.

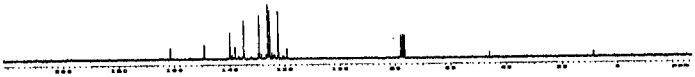

A-8: ^{13}C NMR of $(Et_4N)_2[Co_2(PyPS)_2]$in DMSO on a 200 MHz instrument.

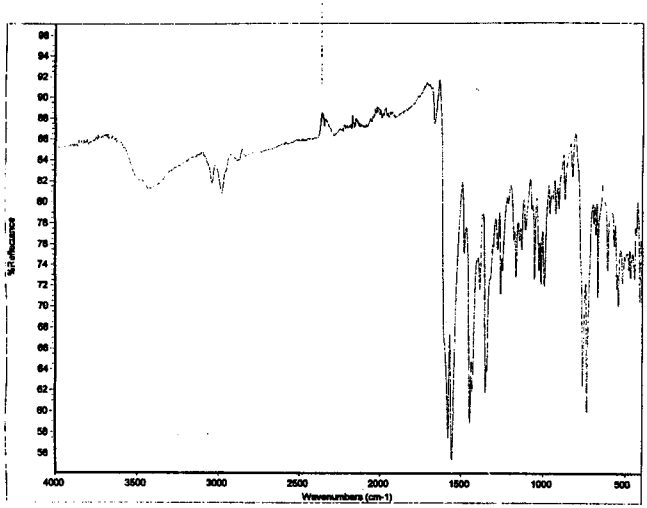

A-9: IR of $(Et_4N)_2[Co_2(PyPS)_2]$.

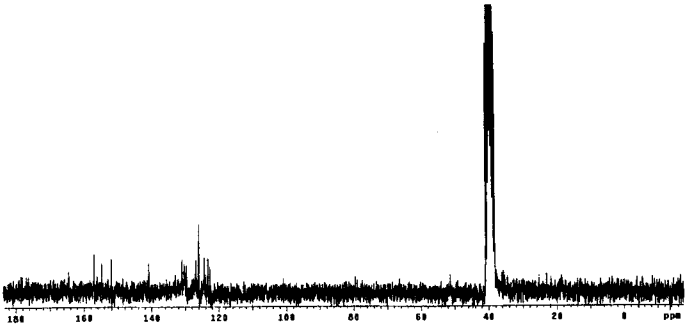

A-10: ^{13}C NMR of $[Co_2(PyPS(SMe))_2]$ in DMSO on a 200 MHz instrument.

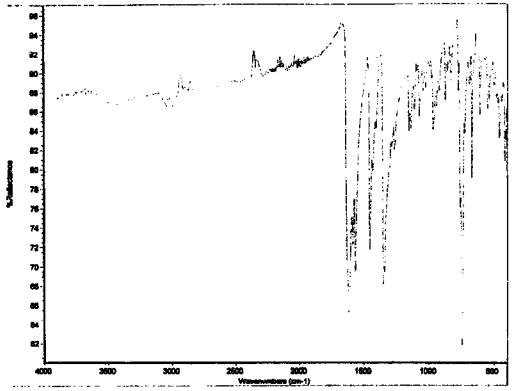

A-11: IR of $[Co_2(PyPS(SMe))_2]$.

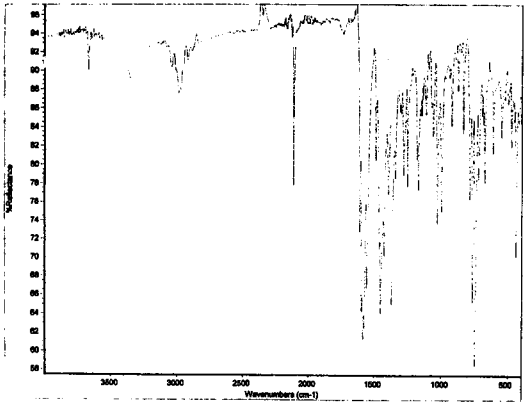

A-12: IR of $[Co_2(PyPS(SMe))_2(^{12}CN)_2]$.

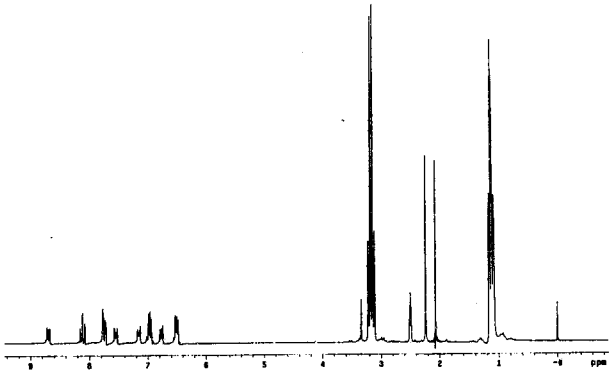

A-13: ^{1}H NMR of $[Co_2(PyPS(SMe))_2(^{13}CN)_2]$ in DMSO on a 200 MHz instrument.

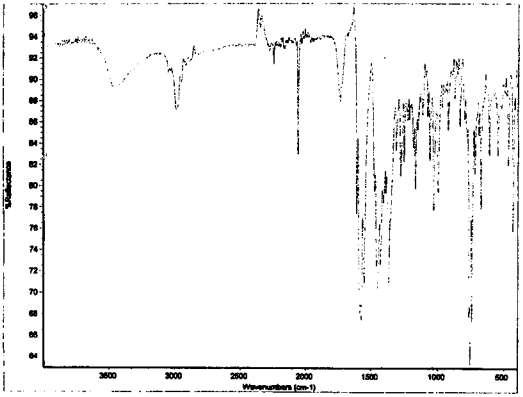

A-14: IR of $[Co_2(PyPS(SMe))_2(^{13}CN)_2]$.

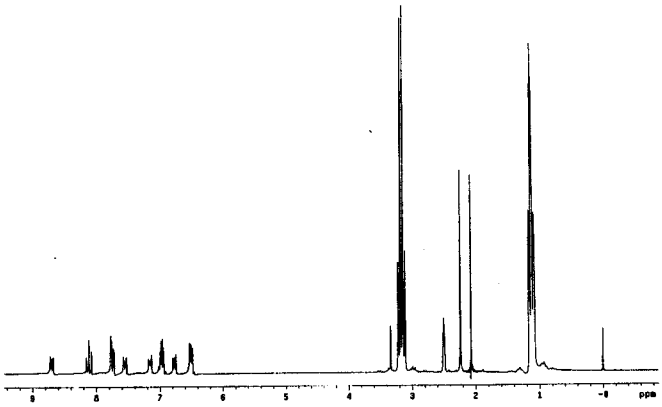

A-15: ^{1}H NMR of 50:50 combined addition $[Co_2(PyPS(SMe))_2(^{13}CN)(^{12}CN)]$ in DMSO on a 200 MHz instrument.

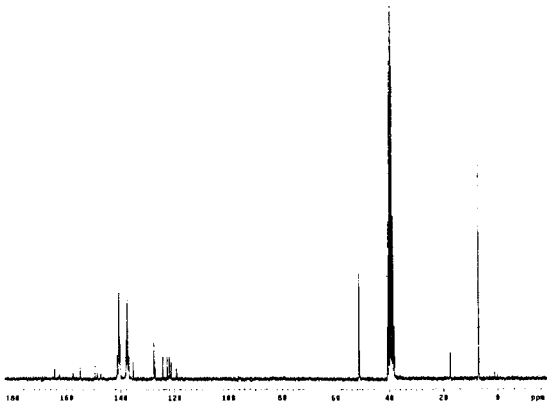

A-16: ^{13}C NMR of 50:50 combined addition $[Co_2(PyPS(SMe))_2(^{13}CN)(^{12}CN)]$ in DMSO on a 200 MHz instrument.

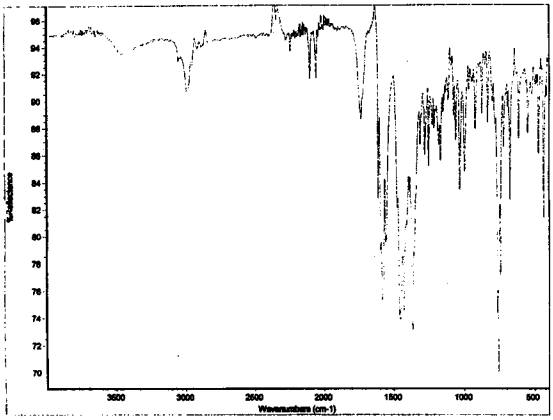

A-17: IR of 50:50 combined addition $[Co_2(PyPS(SMe))_2(^{13}CN)(^{12}CN)]$.

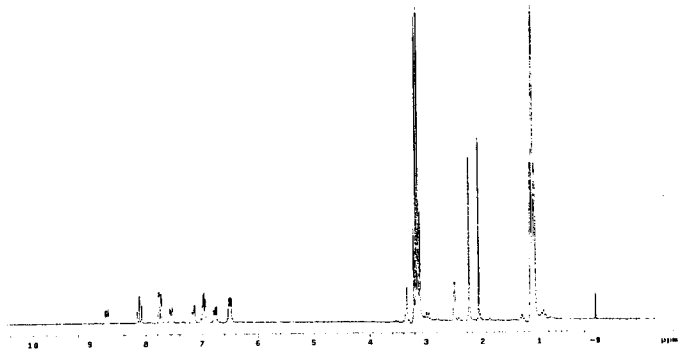

A-18: ^1H NMR of ^{13}CN first $[Co_2(PyPS(SMe))_2(^{13}CN)(^{12}CN)]$ in DMSO on a 200 MHz instrument.

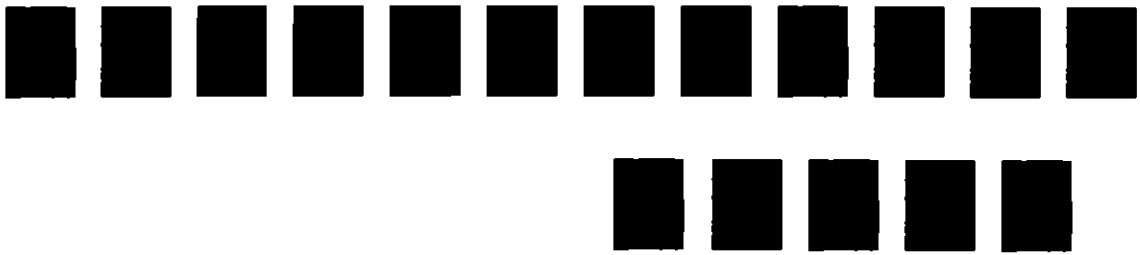

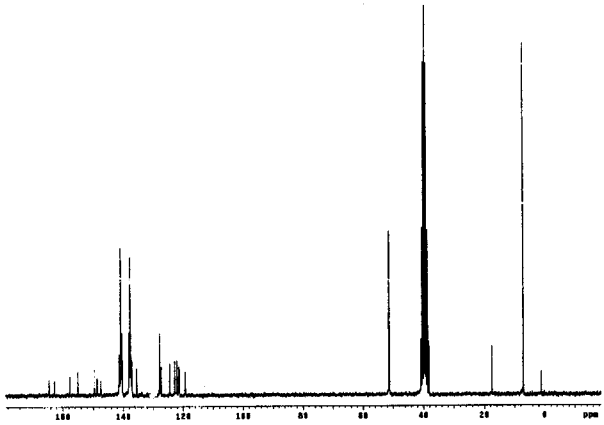

A-19: ^{13}C NMR of ^{13}CN first $[Co_2(PyPS(SMe))_2(^{13}CN)(^{12}CN)]$ in DMSO on a 200 MHz instrument.

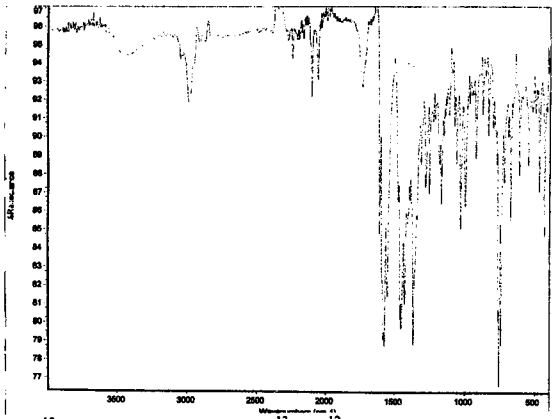

A-20: IR of ^{13}CN first $[Co_2(PyPS(SMe))_2(^{13}CN)(^{12}CN)]$.

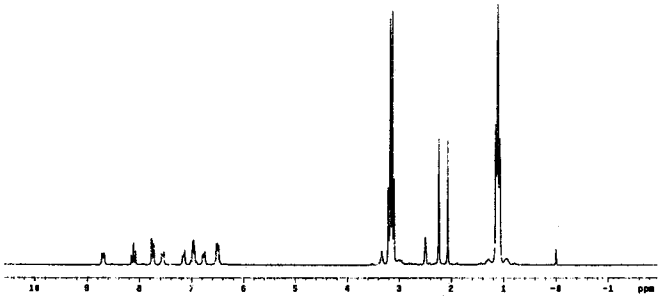

A-21: ^{1}H NMR of ^{12}CN first $[Co_2(PyPS(SMe))_2(^{13}CN)(^{12}CN)]$ in DMSO on a 200 MHz instrument.

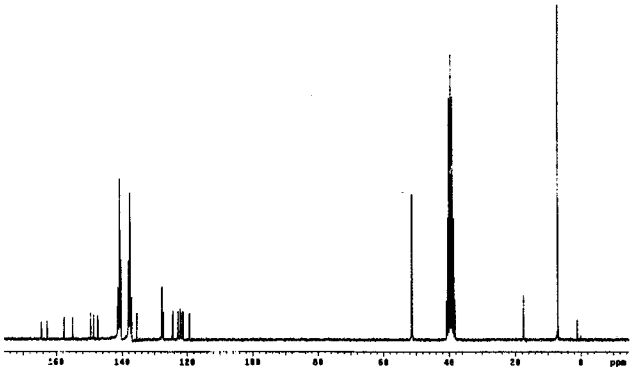

A-22: ^{13}C NMR of ^{12}CN first $[Co_2(PyPS(SMe))_2(^{13}CN)(^{12}CN)]$ on a 200 MHz instrument.

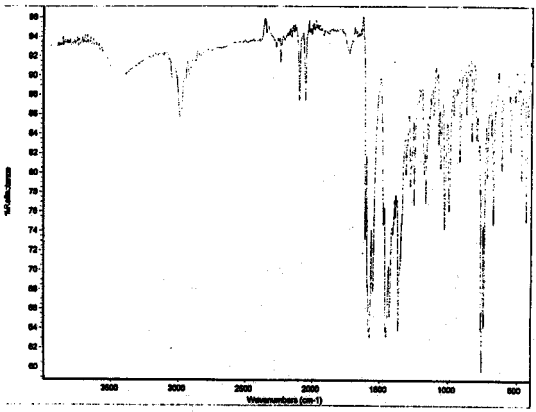

A-23: IR of ^{12}CN first $[Co_2(PyPS(SMe))_2(^{13}CN)(^{12}CN)]$.

Appendix B

❖ Background of Work

This side project involved an attempt to make the dicyano complex from the commercially available Jacobsen's catalyst. As shown if Figure B-1, Jacobsen's catalyst is a chiral complex, in which the two chiral carbon are centers (denoted by the wedge and dash) are off of the cyclohexane ring.

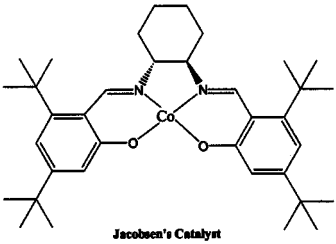

Figure B-1. The structure of Jacobsen's Catalyst.

The tetradentate salen ligand affords two open coordination sites for CN^- to bind in a trans- fashion.

There were many problems that arose when trying to make the dicyano. First, the cobalt in Jacobsen's catalyst is cobalt (II), which is paramagnetic. Upon addition of the CN^-, a concurrent oxidation occurs forming a Co(III) and diamagnetic species. These two features combined made it difficult to isolate pure product.

Because no ^1H NMR spectrum could be obtained for the starting Jacobsen's catalyst, confirmation of the ligation of the two cyanides proved difficult. Also, the

complex as shown in the synthesis section is balanced with one positive charge and would have a negative charged species from the solution as a counterion.

As noted in the NMR spectrum in B-1, there is a very large singlet at 134.5 ppm which corresponds to the cyanide. As observed, this peak is a singlet, meaning that the two cyanides are in equivalent chemical environments. This means that the complex is not asymmetric and no splitting is observed (Figure B-2).

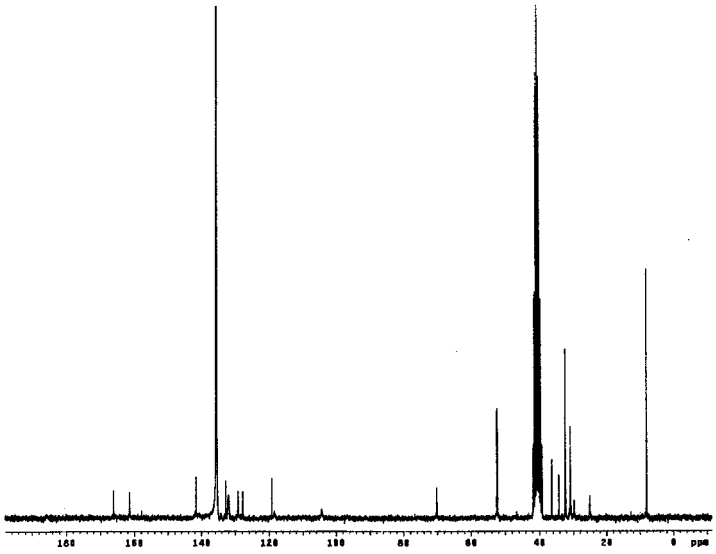

Figure B-2. The ^{13}C NMR of J-Cat$(CN)_2$ in DMSO acquired on a 200 MHz NMR instrument.

❖ **Synthesis**

Attempted synthesis of[J-Cat(CN)$_2$]$^+$

A batch of 0.366 g (0.6062 mmol) Jacobsen's catalyst was dissolved in 175 mL acetone. In a separate vial, 0.208 g (1.334 mmol) NEt_4CN was slurried in 15 mL of acetone. On addition of the cyanide slurry to the Jacobsen's catalyst, the solution changed color to a purple/brown. The reaction was stirred 1.5 h and the acetone was pulled off via rotary evaporation and the solid was recrystalized from ether diffusions from THF.

* The same procedure was also used in the synthesis with DMF. The isotopically labeled cyanide reaction was done in DMF as a solvent.

Appendix C

❖ Background of Work

In this work, done mostly over the summer of 2005, the ligands that were made were those that would force a trans- configuration of the two cyanides. The two ligands that were synthesized are shown below in Figure C-1.

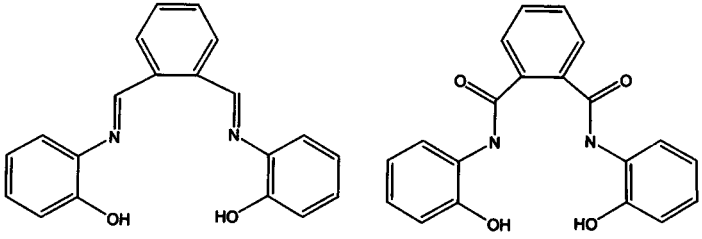

Phenyl Diamine Phenol (PdIP) **Dipeptide Phenol (DPP)**

Figure C-1. Two synthesized tetradentate ligands.

The two ligands above are tetradentate ligands and bind to the four equatorial sites around the cobalt center. The two cyanides would occupy the axial sites in the complex. The dicyano complexes of the above ligands were not attempted before switching directions in the project, although the synthesis of the ligands was accomplished. The dipeptide phenol (DPP) ligand is not observed in the literature.

❖ **Syntheses**

DPP

A batch of 1.00 g (4.93 mmol) phthaloyl dichloride was dissolved in 35 mL of tetrahydrofuran (THF). Next, 1.57 mL (11.330 mmol) of triethylamine was added dropwise to the solution. In a separate flask, 1.047 g (9.852 mmol) of 2-aminophenol was dissolved in 30 mL THF and then added dropwise to the acid chloride solution. The solution was refluxed for 24 h and then the THF was removed via rotary evaporation. The resultant oil was dissolved in chloroform and was washed three times each with 50 mL portions of brine and water. The volume of chloroform was then reduced to 30 mL via rotary evaporation and the solution was cooled to 0°C for 12 h. The white solid was collected via vacuum filtration and dried in vacuo. Yield 0.731 g (42.6 %). ^{1}H NMR (DMSO, 200 MHz) δ from TMS 2.502 (m, DMSO) 3.343 (s, H_2O), 6.948 (m), 7.943 (m), 9.853 (s, NH). Selected IR Bands (v, cm^{-1}): 3373.59 (amide v_{NH}).

PdIP

A 250 mL round bottom flask was charged with 1.00 g (7.46 mmol) phthaldialdehyde and 40 mL of methanol. In a separate beaker, 1.63 g (14.91 mmol) of 2-aminophenol was dissolved in 40 mL of methanol. The 2-aminophenol solution was then added to the phthaldialdehyde solution and the mixture was stirred for 45 min. The total volume of the reaction was then reduced to 50 mL and then 10 mL diethylether was added. The solution was stored at 0 °C for 10 h. The orange precipitate was collected on a Büchner funnel and dried in vacuo. ^{1}H NMR (DMSO, 200 MHz) δ from TMS 2.498 (m, DMSO),

3.339 (s, H_2O), 7.023 (m), 7.450 (m), 7.585 (m) 7.765 (m) 0.491 (s, OH), 9.928 (s, immine NH).

❖ **Spectroscopy**

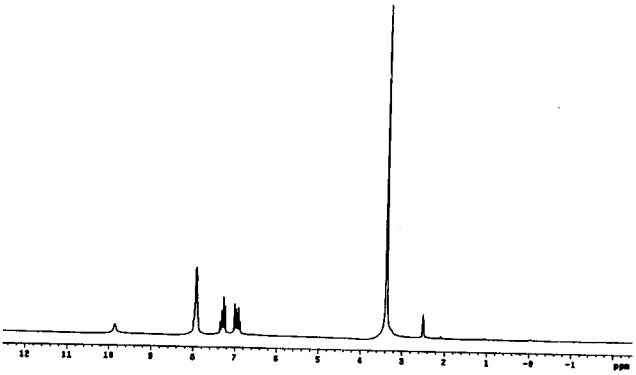

Figure C-2. The ^{13}C NMR of DPP in DMSO acquired on a 200 MHz NMR instrument.

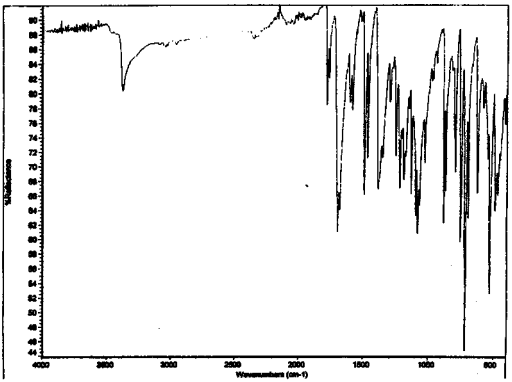

Figure C-3. The IR of DPP.

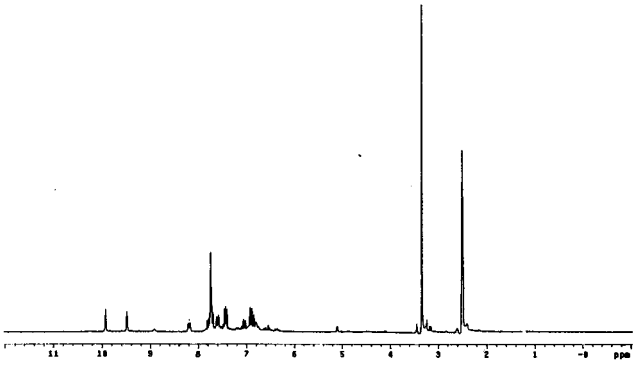

Figure C-4. The ^{1}H NMR of PdIP in DMSO acquired on a 200 MHz NMR instrument.

Appendix D

❖ Background of Work

The purpose of this work was to design a ligand frame which would support the dicyano complex shown in Figure D-1.

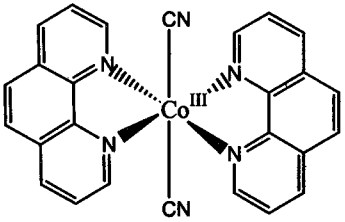

Figure D-1. The Structure of $[Co(Phen)_2(CN)_2]Cl$.

The 1,10-phenanthroline is a bidentate which coordinates to the cobalt metal center through its two nitrogen donors. There were two major steps to this synthesis, the first was to make a tris-1,10-phenanthroline starting material for the dicyano complex. The starting material was then reacted with the cyanide ligands to form the dicyano complex as shown above. The dicyano complex was made with unlabeled ^{12}CN, and ended before a labeled cyanide reaction was attempted. Figuring out what the starting material for the reaction was a challenge in this project as the NMR spectra showed retained solvent which was unable to be removed even after significant time under high vacuum. A crystal structure was then obtained for the starting material and it was found to be tris-1,10-phenanthroline as shown above. The relevant spectroscopy for this project can be found in the spectroscopy section below with the tris-phenanthroline ^1H NMR, ^{13}C NMR,

x-ray crystal structure, and dicyano complex ^{1}H NMR, ^{13}C NMR, and IR respectively. As a note, the peak at -16.7 ppm on D-1 indicates that the complex is cobalt (II) and is paramagnetic. Therefore, there it is harder to get a good NMR as the spins of the unpaired electrons in the complex interfere with the detection of the signals of the proton spins.

❖ **Syntheses**

$[Co(Phen)_3](NO_3)_2$

1.00 g (3.44 mmol) of $Co^{II}(NO_3) \cdot 6H_2O$ was dissolved in 40 mL of ethanol. In a separate beaker, 2.170 g (12.040 mmol) of 1,10-phenanthroline were dissolved in 25 mL of ethanol. The 1,10-phenanthroline solution was then added to the cobalt solution resulting in a clear, orange-yellow solution. After 30 min, a yellow precipitate formed which was collected via vacuum filtration. The solid was washed two times with 15 mL portions of acetone and air dried. Crystals suitable for x-ray analysis were obtained by slow diffusion of diethylether into an ethanol solution of the solid. ^{1}H NMR (DMSO, 200 MHz) δ from TMS: 1.077 (t), 3.449 (q), 4.341 (t), 7.780 (m, phen), 8.032 (m, phen), 8.549 (m, phen), 9.001 (m, phen). ^{13}C NMR (DMSO, 50.3 MHz) δ from TMS: 19, 59, 125.392, 127.274, 129.254, 130.476, 137.388, 141.538, 147.456, 197.700.

$[Co(Phen)_2(CN)_2]Cl$

A batch of 0.1833 g (1.173 mmol) of NEt_4CN was dissolved 3 mL of dry ethanol. In a separate beaker, 300 mg (0.587 mmol) of $[Co(phen)_3](NO_3)_3$ was dissolved in 40 mL

ethanol. The cyanide solution was then added drop wise to the $[Co(phen)_3](NO_3)_3$ solution. After 10 h, a brown-yellow precipitate formed and was collected and dried under vacuum. ^1H NMR (DMSO, 200 MHz) δ from TMS 7.631 (d, phen), 7.829 (q, phen), 8.529 (m, phen), 8.972 (d, phen), 9.295 (d, phen), 9.650 (d, phen). ^{13}C NMR (DMSO, 50.3 MHz) δ from TMS 127.524, 128.055, 128.328, 128.867, 130.559, 131.029, 140.096, 140.969, 144.937, 146.113, 150.560, 155.947. Selected IR Bands (ν, cm^{-1}): 2140.84 (ν_{CN}).

$[Co(phen)_2(^{13}CN)_2]Cl$

The ^{13}C labeled CN complex was synthesized in the same manner as the unlabeled listed above. The spectra are identical to the unlabeled spectra.

❖ **Spectroscopy**

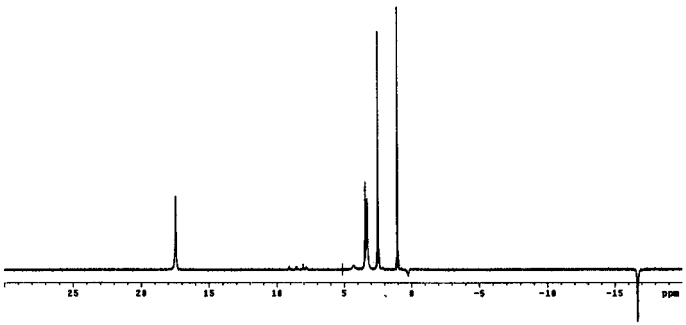

Figure D-2. The ^1H NMR spectrum of $[Co(Phen)_3](NO_3)_2$ in DMSO on a 200 MHz instrument.

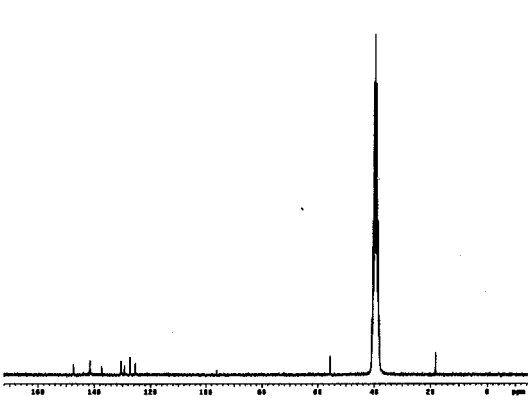

Figure D-3. The ^{13}C NMR spectrum of $[Co(Phen)_3](NO_3)_3$ in DMSO on a 200 MHz instrument.

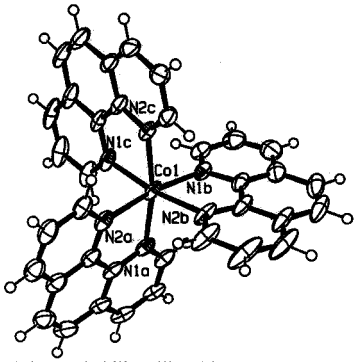

ORTEP diagram (50% probability ellipsoids)

Figure D-4. The crystal structure of $[Co(Phen)_3](NO_3)_3$.

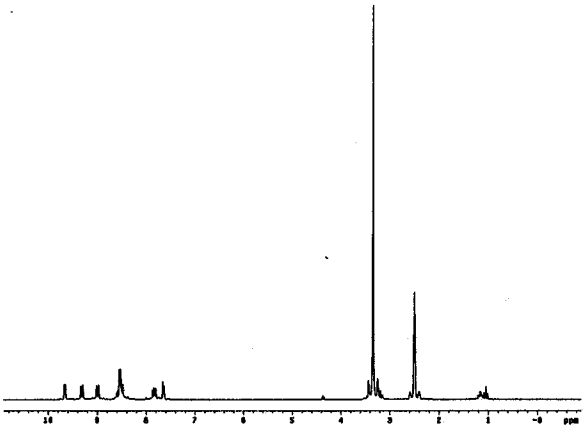

Figure D-5. The ^{1}H NMR spectrum of $[Co(phen)_2(^{13}CN)_2]Cl$ in DMSO on a 200 MHz instrument.

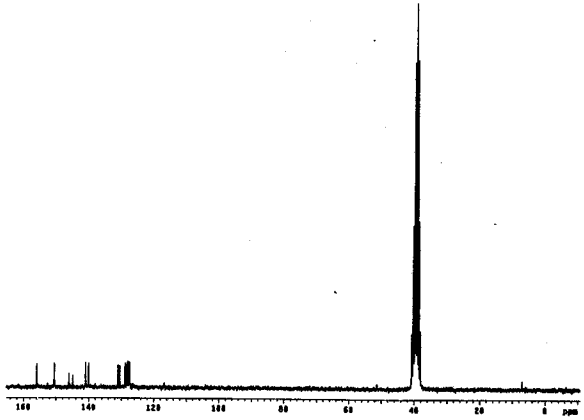

Figure D-6. The ^{13}C NMR of $[Co(phen)_2(^{13}CN)_2]Cl$ in DMSO on a 200 MHz instrument.

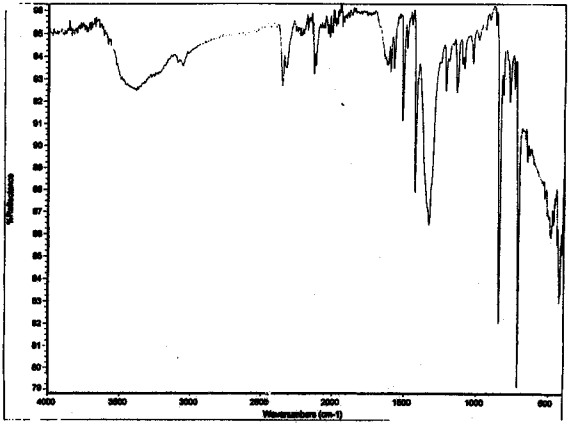

Figure D-7. The IR of the $[Co(phen)_2(^{13}CN)_2]Cl$.

References

1. Paulder, W. W. *Nuclear Magnetic Resonance General Concepts and Applications*; John Wiley & Sons, Inc: New York, NY, 1987, 1-68.
2. Becker, E. D. *High Resolution NMR Theory and Chemical Applications;* Second Edition; Academic Press: New York, NY, 1980, 85-102.
3. Skoog, D. A., Holler, J. F., Nieman, T. A. *Principles of Instrumental Analysis;* Fifth Edition; Thompson Learning Inc. Toronto, Ontario, 1998, 445-498.
4. T. Pochapsky, S. Pochapsky, Current Topics in Medicinal Chemistry, 1 (2001) 427.
5. Patrick, Graham L. *An Introduction to Medicinal Chemistry;* Second Edition; Oxford University Press: New York, NY, 2004, 152-153, 167-169, 211, 170, 304, 403, 574.
6. Braunstein, P., Rose, J. Organometallics 10 (1991) 3686.
7. Young, S. W. *Nuclear Magnetic Resonance Imaging Basic Principles;*Raven Press: New York, NY, 1984, ix-10.
8. Shriver, D. F., Atkins, P. W. *Inorganic Chemistry*; Third Edition; W.H. Freeman and Company: New York, NY, 2003, 659-661.
9. C. Boyke, J. Van Der Vlugt, T. Rauchfuss, S. Wilson, G. Zampella, G.L. De Gioia, J. Am. Chem. Soc. 127 (2005) 11010.
10. T. Kurahashi, Y. Kobayashi, S. Nagatomo, T. Tosha, T. Kitagawa, H. Fujii, Inorg. Chem. 44 (2005) 8156.
11. Fujii, H. J. Am. Chem. Soc. 124 (2002), 5936.
12. Noveron, J. C., Olmstead, M. M., Mascharak, P. K. J. Am. Chem. Soc. 123 (2001) 3247.
13. Tyler, L. A., Noveron, J. C., Olmstead, M. M., Mascharak, P. K., Inorg. Chem. 42 (2003) 5751.
14. Tyler, L. A., Olmstead, M. M., Mascharak, P. K. Inorg. Chim. Acta. 321 (2001) 135.